

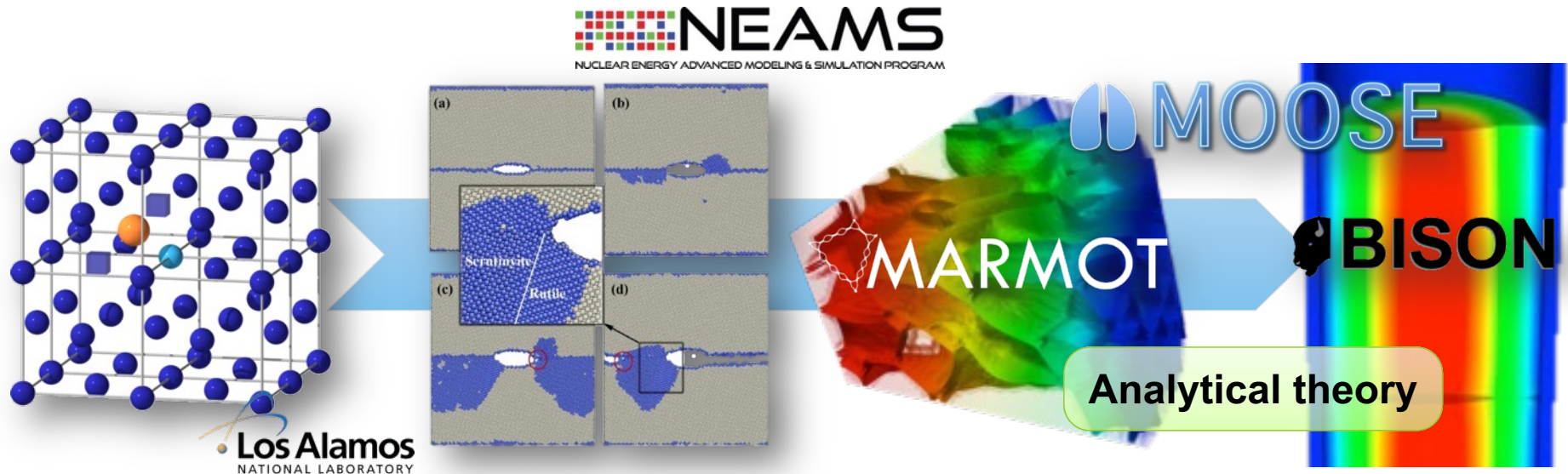
Phase-field simulations to inform nuclear fuel performance modeling

Larry Aagesen
Idaho National Laboratory

Co-authors/Colleagues:
Wen Jiang, Sudipta Biswas, Al Casagrande, Steve Novascone, Kyle Gamble
Idaho National Laboratory
David Andersson, Michael Cooper, Topher Matthews
Los Alamos National Laboratory

Multiscale fuel performance simulation

- BISON: Fuel performance code developed at INL
- Inform BISON with atomistic and mesoscale simulations
 - Marmot: MOOSE-based phase-field simulation code



nanometers

First Principles

- Identify critical bulk mechanisms
- Determine bulk properties

100's of nanometers

Molecular Dynamics

- Identify interfacial mechanisms
- Determine interfacial properties

microns

Mesoscale

- Predict microstructure evolution
- Determine impact on properties

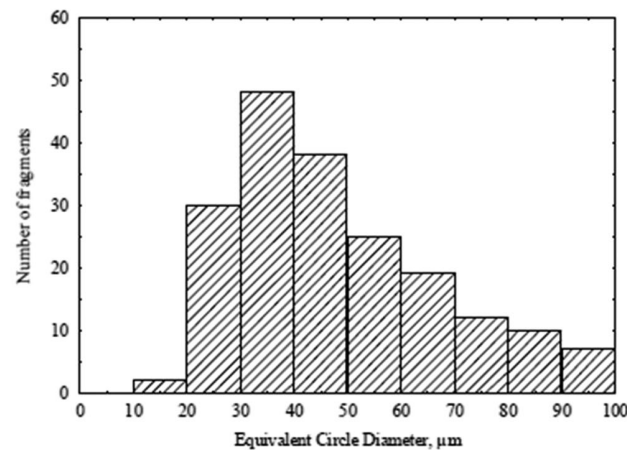
millimeters and up

Engineering Scale

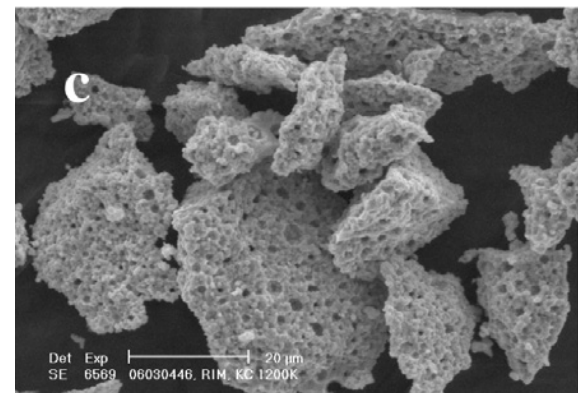
- Use analytical theory
- Predict fuel performance

Fine fragmentation/pulverization of high-burnup UO₂

- Potential to occur during loss-of-coolant accident (LOCA)-type temperature transients
- Formation of fine fragments <100 micron in size
- Fine particles can potentially escape into coolant from burst cladding during LOCA
- Industry would like to understand this problem better to strengthen their case for increasing fuel burnup limit from 62 to 75 GWd/MTU
- Hypothesized mechanism: During LOCA, trapped gas in bubbles heats up and becomes overpressurized; cracking initiates at these overpressurized bubbles

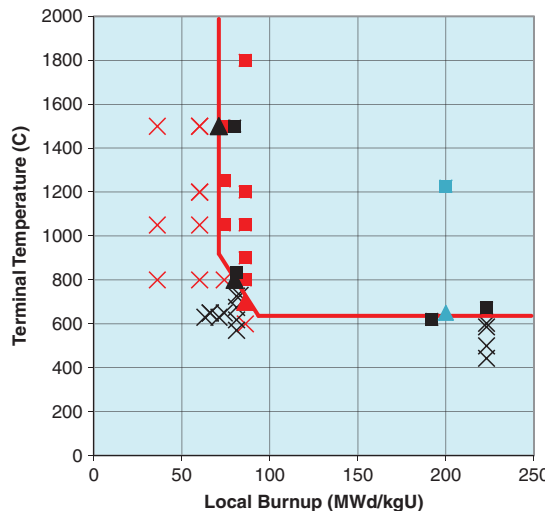


Turnbull et al., Nuc. Sci. & Eng., 179,477 (2015).

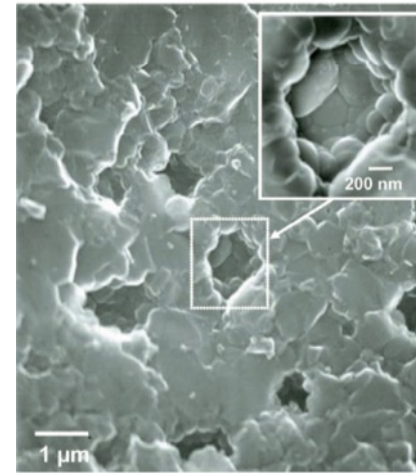


Hiernaut et al, JNM 377, 313 (2008).

BISON model for pulverization



Turnbull et al., Nuc. Sci. & Eng., 179,477 (2015).

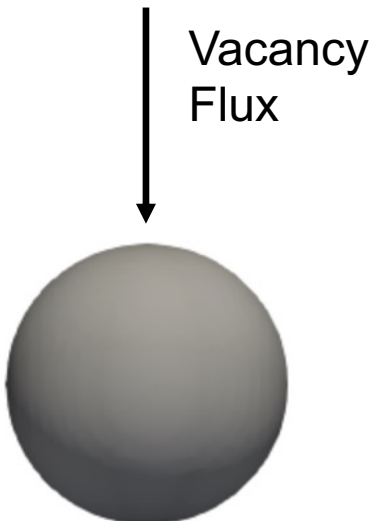


High-burnup structure in UO₂
[Sonoda et al., NIMB, 2002].

- Current model is empirical, based on burnup and temperature
- Pulverization is predominantly observed to occur in regions where high-burnup structure (HBS) has partially or completely formed
 - HBS: Grain size decreases to ~150–200 nm, micron-sized bubbles form with multiple grains intersecting each bubble
- Goal: Develop a physics-based criterion for pulverization in BISON that accounts for microstructure
 - Focus on HBS

HBS bubble response to LOCA transient

- Bubbles in HBS region are $\sim 1 \mu\text{m}$ and believed to be overpressurized relative to equilibrium (based on observed dislocation punching around bubbles):
 - $P = \frac{2\gamma_{st}}{R} + \sigma_H$
- Overpressurized bubbles exert compressive stress in the radial direction on the surrounding matrix.
- During LOCA transient, temperature and therefore bubble pressure increases further, causing stress in the matrix to increase further. Compressive stress leads to increased vacancy flux to bubble, causing bubble growth.
- **Key Questions:**
 - Does significant bubble growth occur during duration of a LOCA transient?
 - What is the pressure response to a given temperature transient?

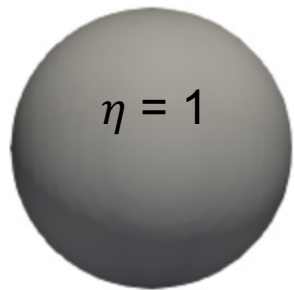


Phase-field model: Essential physics

- Single order parameter η to represent gas bubble and fuel matrix phase
 - Current model does not consider grain boundaries
- Track vacancies and fission product gas atoms
 - Use Xe properties for fission product gases
 - Source terms for production, sink term to limit vacancy concentration to steady-state
- Chemical and elastic energy contributions
- Solid-bubble interfacial energy
 - Kim-Kim-Suzuki (KKS) approach to remove bulk energy contribution to interfacial energy
- Surface tension of bubble-matrix interface
- Xe gas pressure

$$\eta = 0$$

$$\eta = 1$$



Phase-field model: Free energy functional

$$F = \int_V \left[f_{chem} + Wg(\eta) + \frac{\kappa}{2} |\nabla \eta|^2 + f_{el} \right] dV,$$

- f_{chem} = bulk chemical free energy density. $h(\eta)$ is a smooth interpolation function:

$$f_{chem} = [1 - h(\eta)] f_{chem}^m(c_v^m, c_g^m) + h(\eta) f_{chem}^b(c_v^b, c_g^b)$$

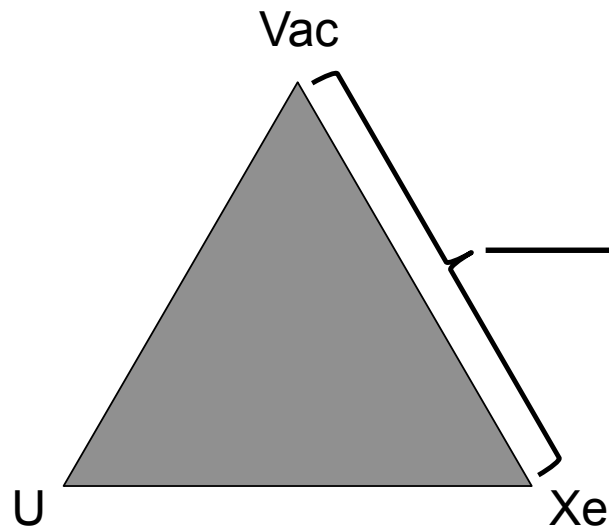
- f_{chem}^m = chemical free energy of the matrix phase. Fit a parabolic approximation to ideal solution energetics:

$$f_{ideal}^m \approx f_{chem}^m = \frac{k_v^m}{2} (c_v^m - c_v^{m,min})^2 + \frac{k_g^m}{2} (c_g^m - c_g^{m,min})^2$$

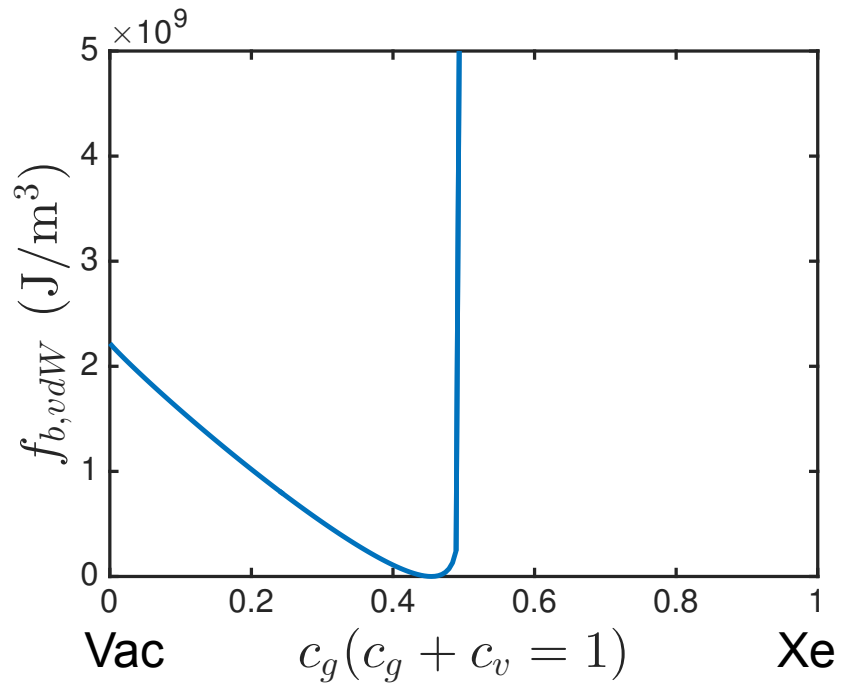
- f_{chem}^b = chemical free energy of the bubble phase. The bubble is considered to be a mixture of gas atoms and U-site vacancies. Energy given by the Helmholtz free energy of a van der Waals gas:

$$f_{chem}^b = c_g^b \frac{kT}{V_a} \left[\ln \left(\frac{1}{n_Q \left(\frac{V_a}{c_g^b} - b \right)} \right) - 1 \right] + \frac{k_p}{2} (1 - c_v^b - c_g^b)^2 + f_0$$

Parameterization for Xe gas phase



Gibbs triangle: U lattice sites



Helmholtz free energy density: Van der Waals gas

Phase-field model: Elastic energy

- Interpolating elastic energies and stresses (Voigt-Taylor scheme):

$$f_{el} = [1 - h(\eta)]f_{el}^m + h(\eta)f_{el}^b \quad f_{el}^m = \frac{1}{2}C_{ijkl}^m \epsilon_{ij}^{el,m} \epsilon_{kl}^{el,m} \quad f_{el}^b = \frac{1}{2}C_{ijkl}^b \epsilon_{ij}^{el,b} \epsilon_{kl}^{el,b}$$

- Mechanical equilibrium equation:

$$\nabla \cdot \sigma_{ij} = \nabla \cdot [(1 - h(\eta))\sigma_{ij}^m + h(\eta)\sigma_{ij}^b + \sigma_{ij}^{st}] = 0 \quad \sigma_{ij}^m = C_{ijkl}^m \epsilon_{kl}^{el,m}$$

- Eigenstrain due to vacancies:

$$\epsilon_{ij}^{el,m} = \epsilon_{ij} - \epsilon_{ij}^* = \epsilon_{ij} - (c_v - c_v^0)\epsilon_v^0 \delta_{ij}$$

- Bubble pressure:

$$\sigma_{ij}^b = - \left(\frac{kT}{\frac{V_a}{c_g^b} - b} \right) \mathbf{I} + C_{ijkl}^b \epsilon_{kl}^{el,b}$$

- Surface tension:

$$\sigma_{ij}^{st} = \left[Wg(\eta) + \frac{\kappa}{2} |\nabla \eta|^2 \right] \mathbf{I} - \kappa \nabla \eta \otimes \nabla \eta$$

Evolution equations

- Allen-Cahn for order parameter:

$$\begin{aligned}\frac{\partial \eta}{\partial t} &= -L \left(\frac{\delta F}{\delta \eta} \right) \\ &= L \left[\frac{dh}{d\eta} \left[(f_T^m - f_T^b) - \mu_v(c_v^m - c_v^b) - \mu_g(c_g^m - c_g^b) \right] - W \frac{dg}{d\eta} + \kappa \nabla^2 \eta \right]\end{aligned}$$

- Cahn-Hilliard for vacancy and gas concentration (source for vacancies and gas atoms, sink for vacancies to approximate recombination):

$$\frac{\partial c_v}{\partial t} = \nabla \cdot M_v \nabla \mu_v + s_v - K_v c_v^m$$

$$\frac{\partial c_g}{\partial t} = \nabla \cdot M_g \nabla \mu_g + s_g$$

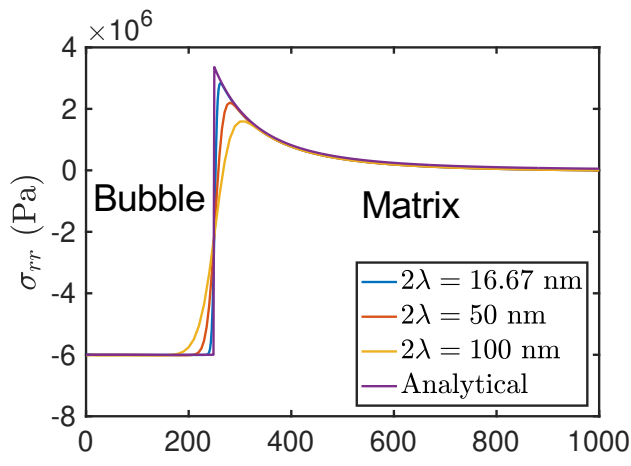
- Mobilities are a function of defect diffusivities:

$$M_g = \frac{h D_g^b + (1-h) D_g^m}{d^2 f / dc_g^2} \quad M_v = \frac{h D_v^b + (1-h) D_v^m}{d^2 f / dc_v^2}$$

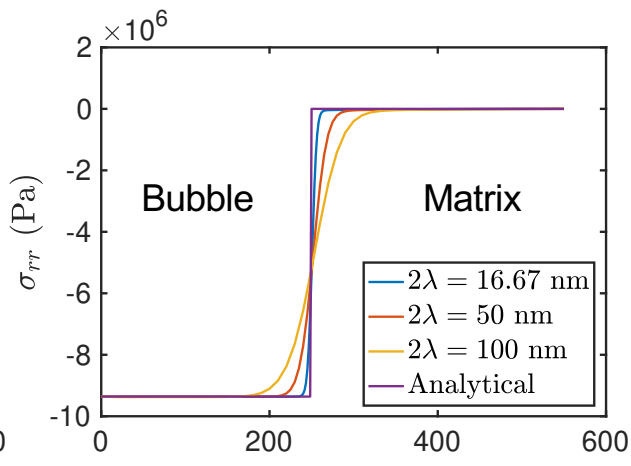
- + KKS system constraints

Phase-field model verification and testing

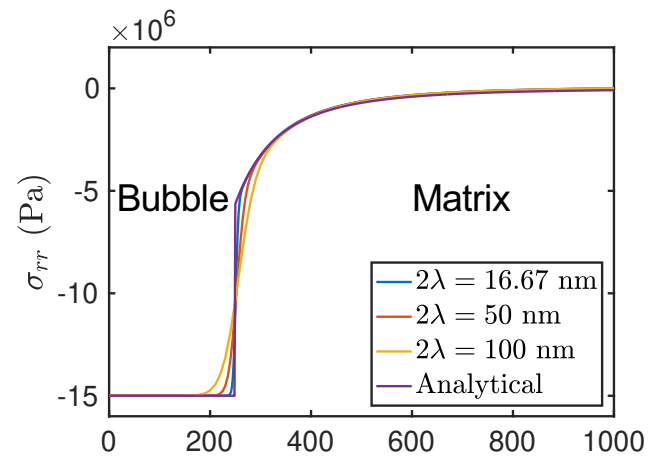
- Considered stress state in equilibrium, underpressurized, overpressurized bubbles (1D simulation in radial coordinates)
 - Equilibrium: $\sigma_{rr} = 0$ in surrounding solid matrix
 - Under/overpressurized: $\sigma_{rr} = +/-$, corresponding to tensile/compressive stress in surrounding matrix
 - Converge to analytical solution as interface width (2λ) decreases



Underpressurized

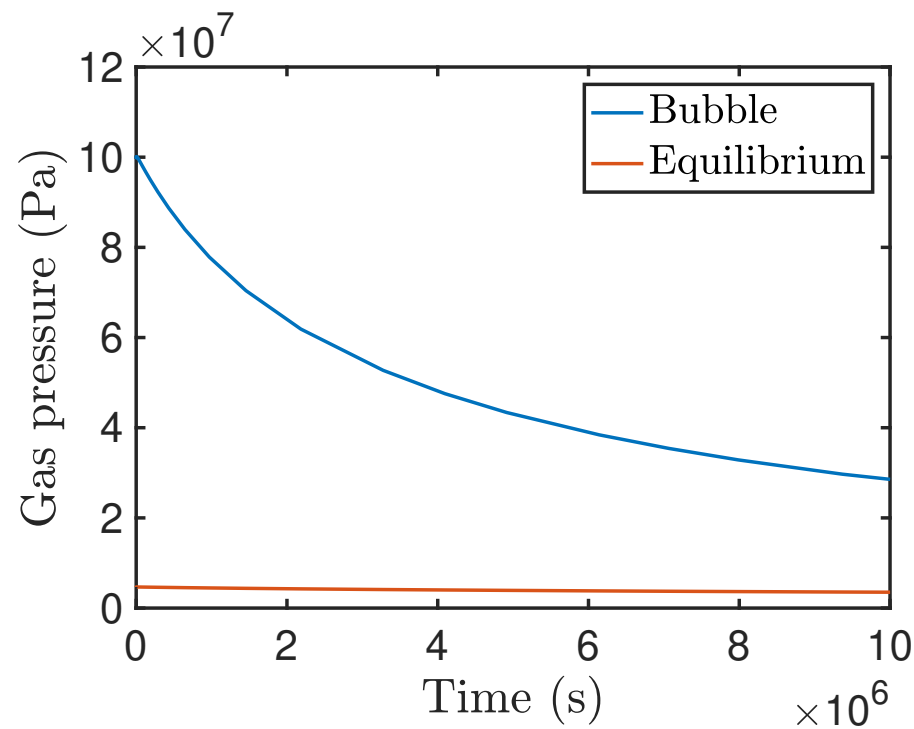
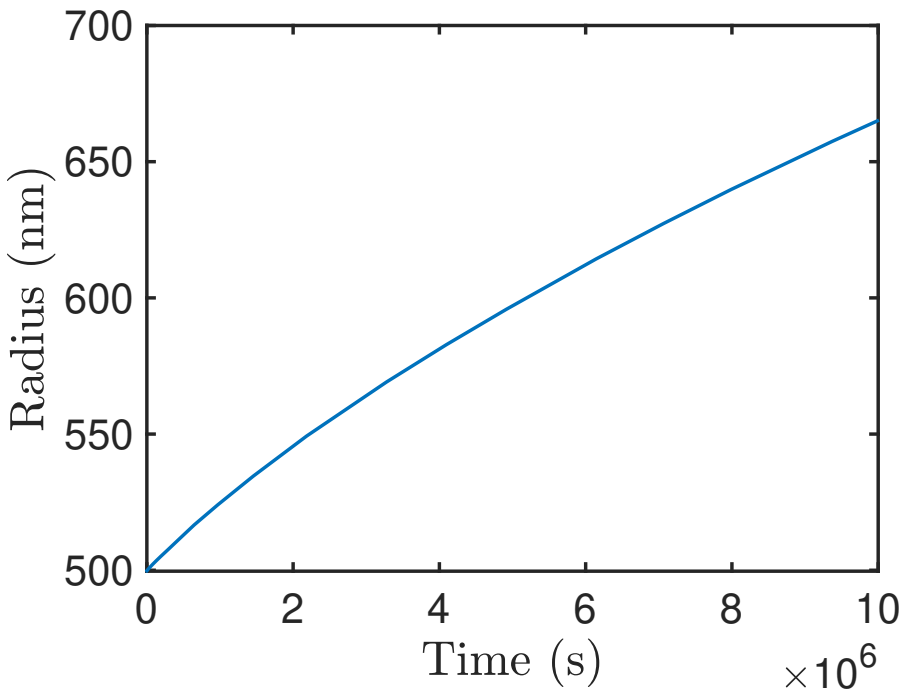


Equilibrium



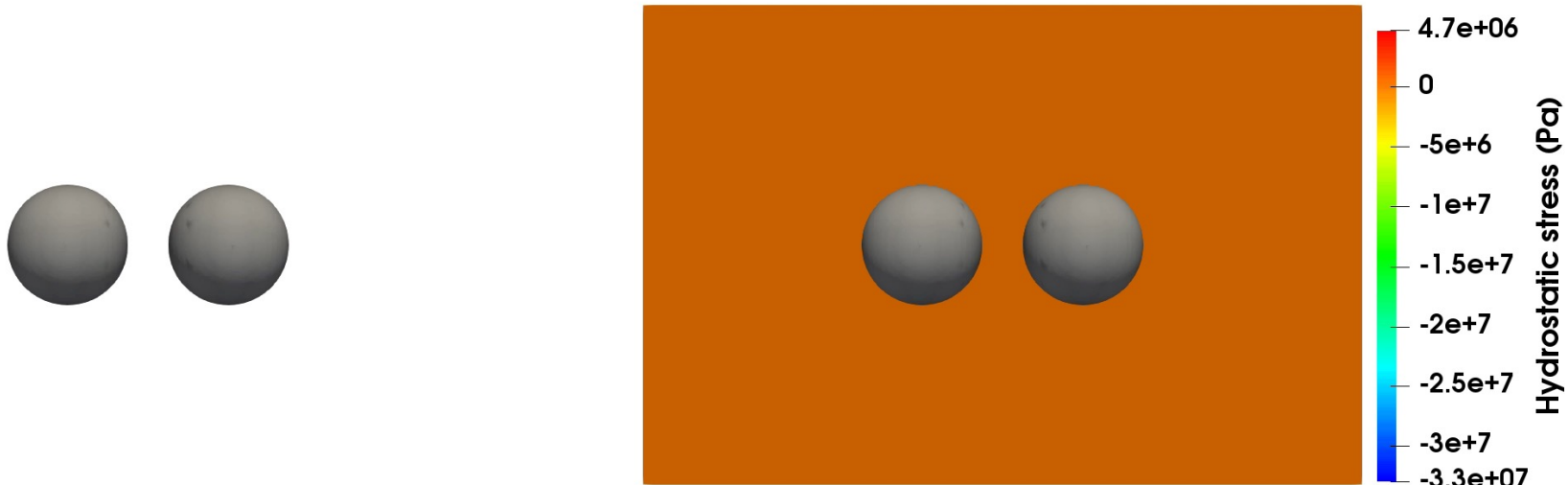
Overpressurized

Bubble growth during steady-state operation

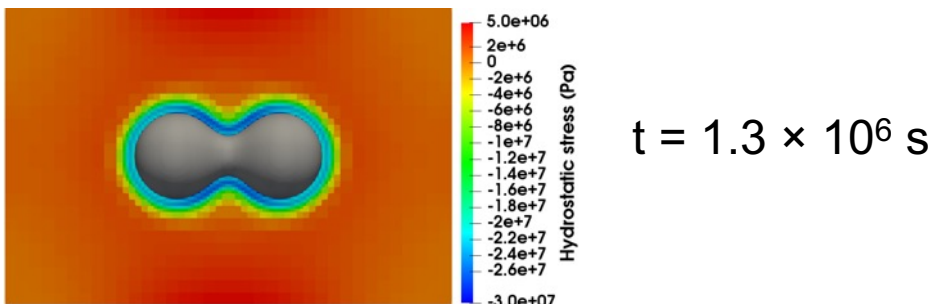


- Assume bubble pressure is 100 MPa in initial conditions
 - Upper bound based on dislocation punching pressure
- Bubble pressure decreases during growth but remains well above equilibrium pressure
 - Increased likelihood of fragmentation during LOCA

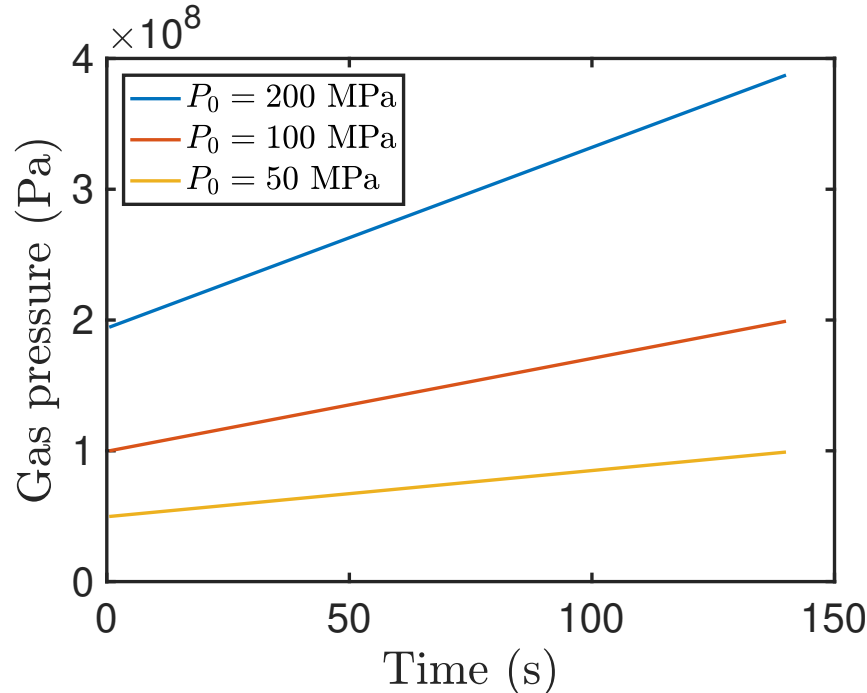
Bubble growth during steady-state operation



- 3D simulation to 1.5×10^7 s, 2 bubble impingement, initial radii of 300 nm
- Hydrostatic stress surrounding bubbles
 - Region of enhanced compressive hydrostatic stress in “neck”

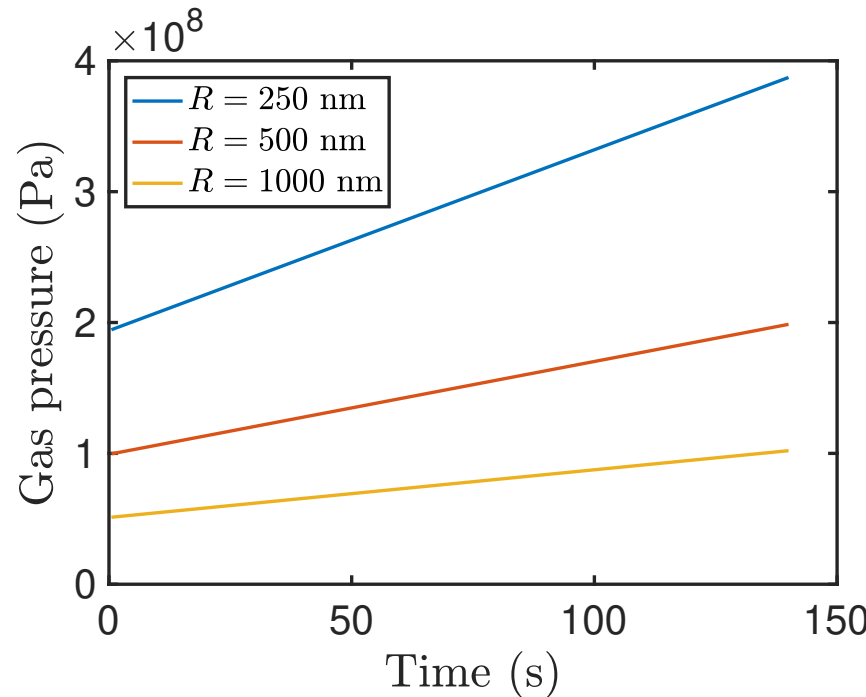


Bubble response during LOCA transient



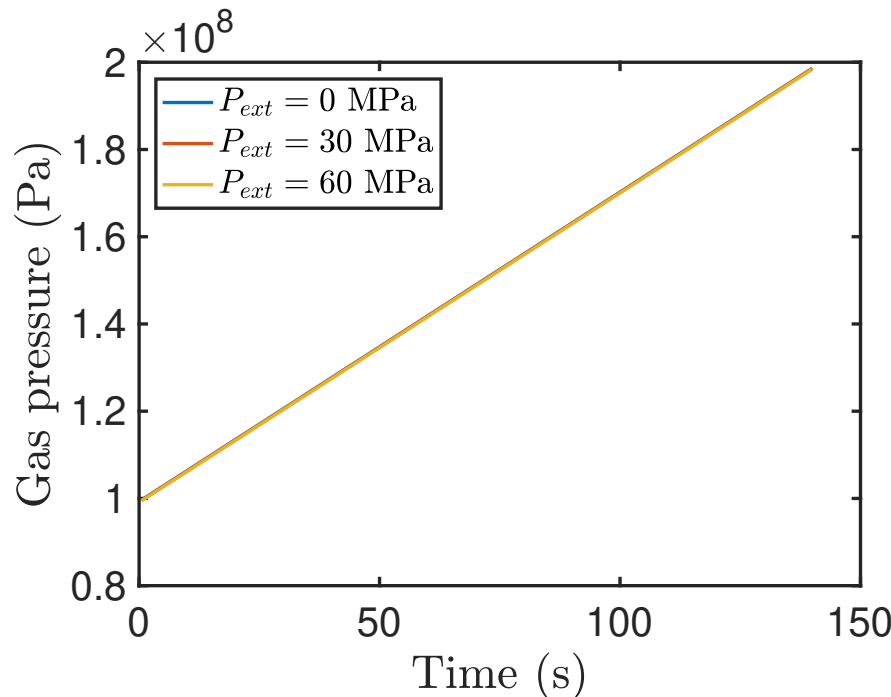
- Temperature ramp from 700 to 1400 K at 5 K/s
- Consider fixed bubble radius of 250 nm in initial conditions
- Maximum initial pressure set to $P_0 = 200 \text{ MPa}$ (upper bound based on dislocation punching); vary P_0 for fixed bubble size
- No significant change in bubble radius for each case

Bubble response during LOCA transient



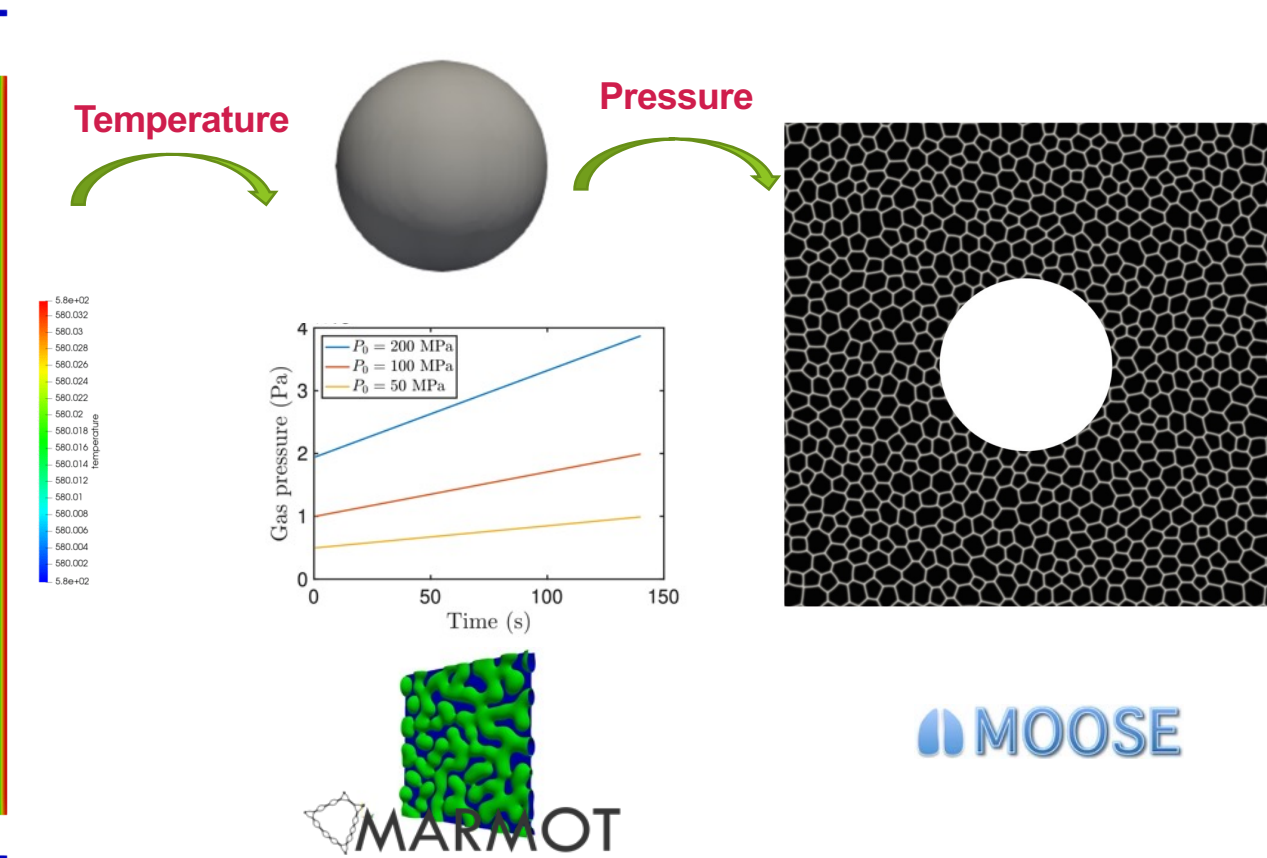
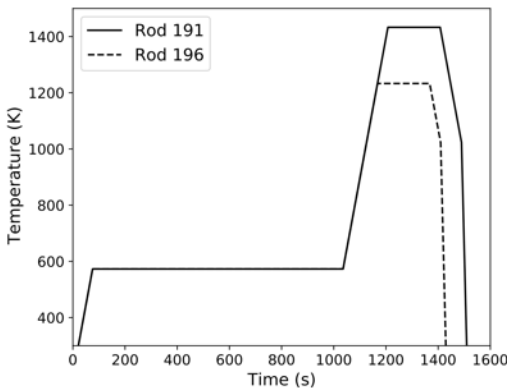
- Vary initial radius: 250 nm, 500 nm, 1000 nm
 - Change domain size to maintain 10% porosity
- Initial pressures set at upper bound estimate from dislocation punching: 200, 100, 50 MPa.
- No significant change in bubble size

Bubble response during LOCA transient



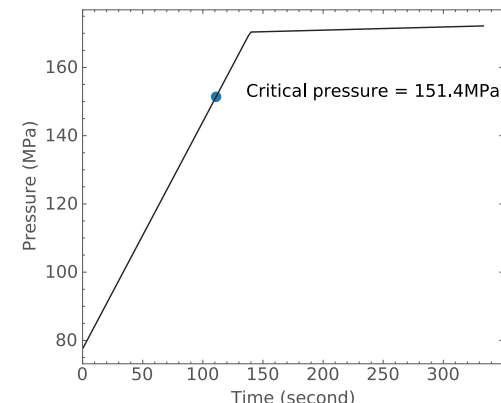
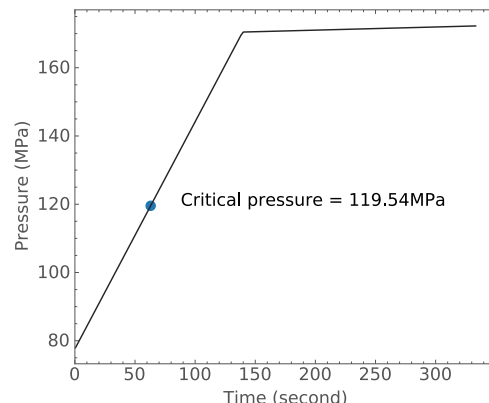
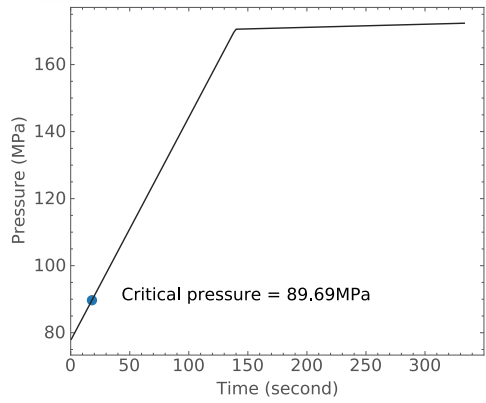
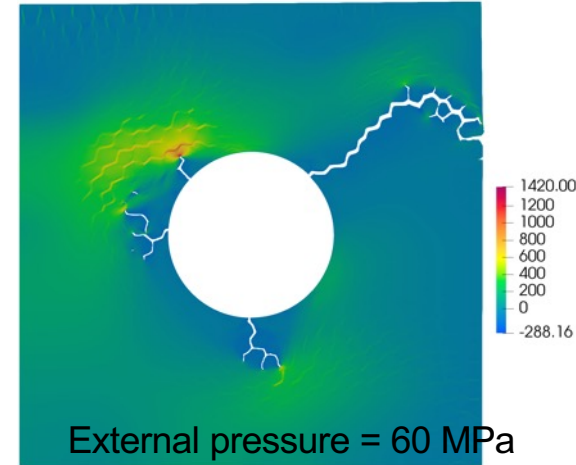
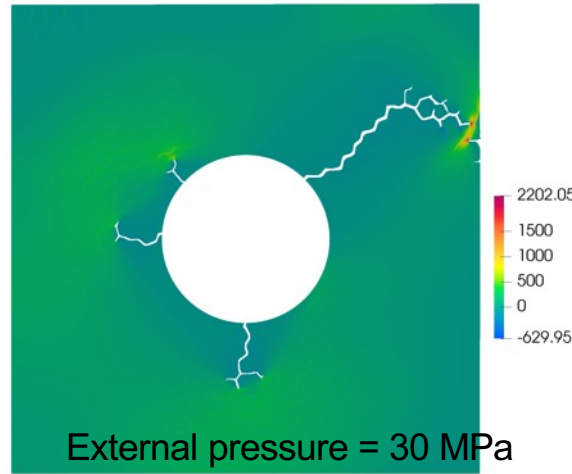
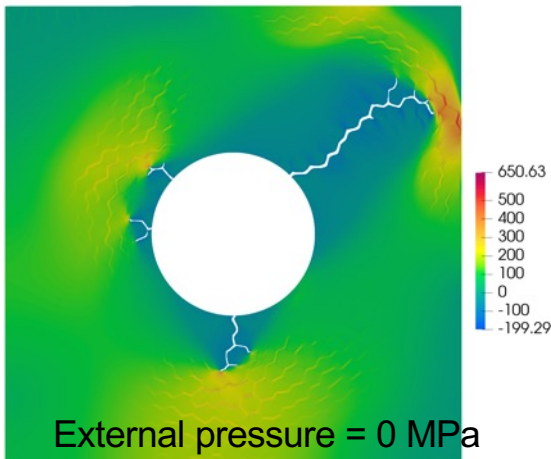
- Vary external pressure at simulation domain boundary, P_{ext} , for constant bubble $R = 500$ and $P_0 = 100 \text{ MPa}$
- No significant size change; pressure transient unchanged
- P_{ext} may have a stronger impact on fracture behavior

Modeling fragmentation in high-burnup UO₂ using phase-field fracture



External pressure

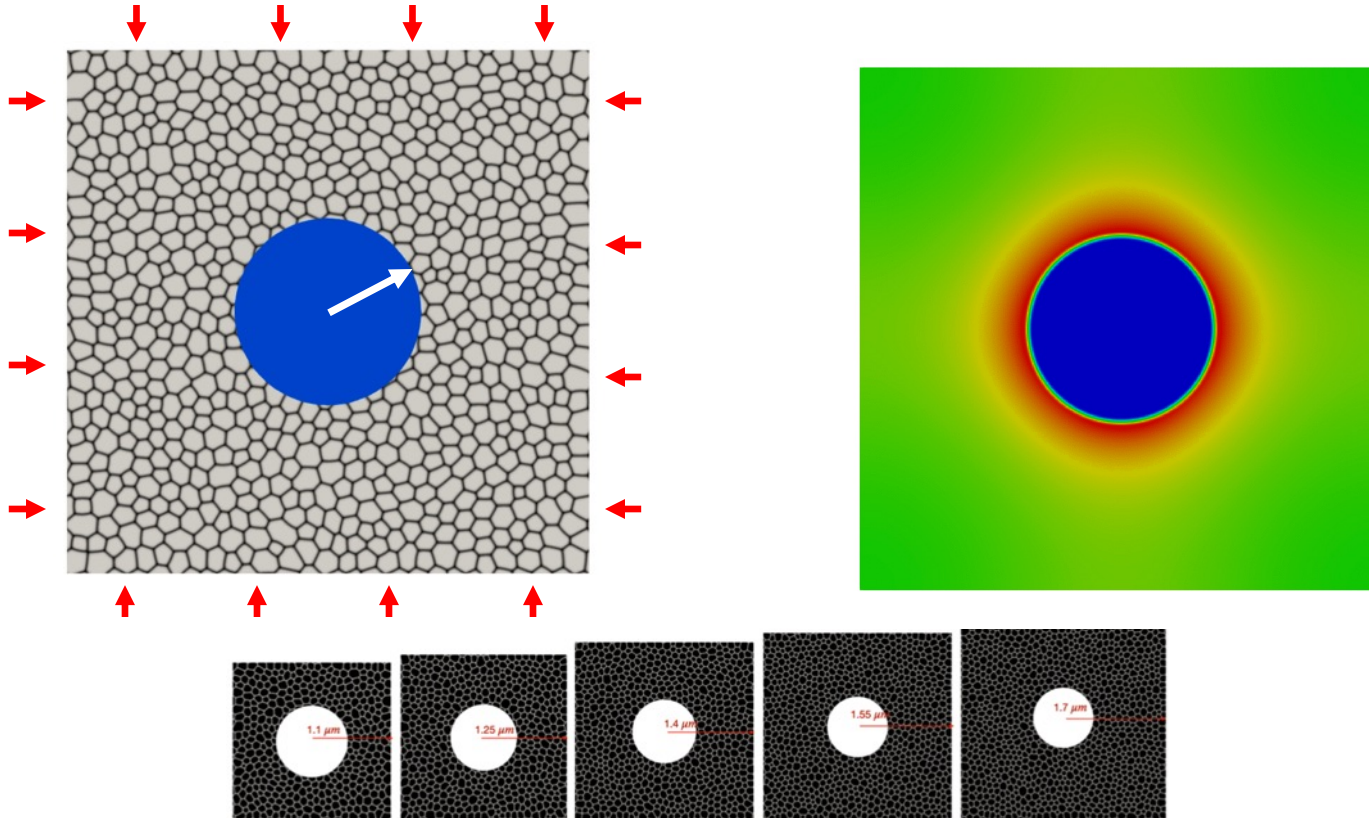
- External restraint pressure significantly affects the gas pressure at which fracture occurs



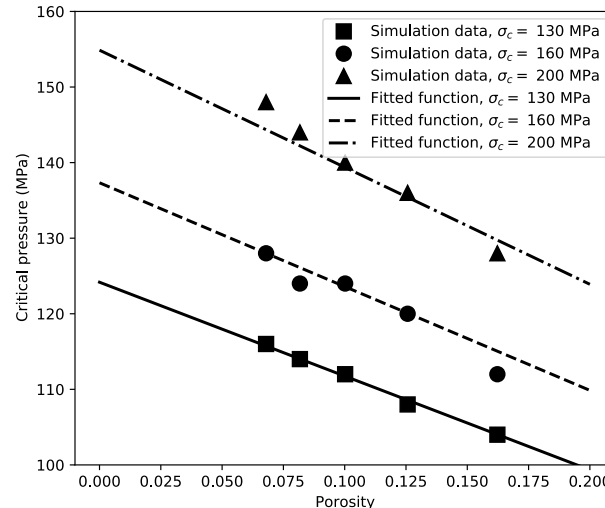
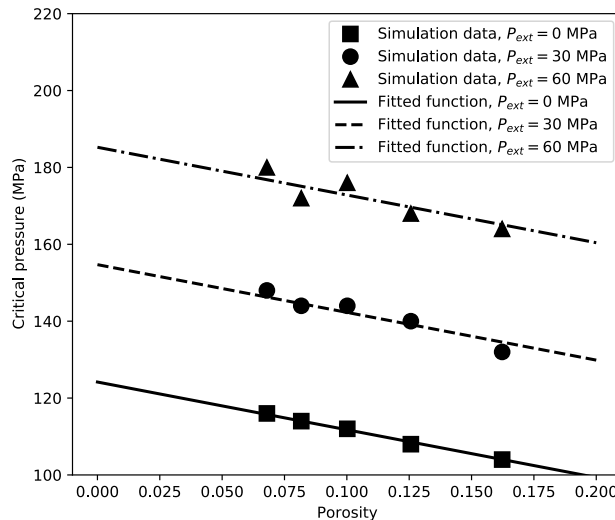
Determine BISON pulverization criterion based on phase-field modeling

Phase-field fracture model was used to inform pulverization criterion for BISON models

- Use periodic boundary conditions to account for multi-bubble interaction.
- Consider varying porosity (p), external pressure (p_{ext}), critical fracture stress of grain boundary (σ_c)



BISON pulverization criterion



- Function to fit the data (a , b , c are fitting constants) :
 - $P_g^{cr} = [a + b(\sigma_{cr} - 130)](1 - p) - cP_{ext}$
- Implemented in BISON. Validation with BISON assessment cases is in progress, using both analytical and phase-field fracture-based criteria
- Future work:
 - Inform fracture model from atomistic simulations (LANL) and experiment (AFC)
 - Consider multi-bubble effects, partial HBS formation

Conclusions: High-burnup UO₂ response to LOCA transients

- Developed new phase-field model that accounts for effects of surface tension and gas bubble pressure to understand non-equilibrium bubbles
- Bubble size did not change significantly during LOCA transients
- Pressure as a function of time determined for given transients and passed to phase-field fracture model
- Developed pulverization criterion in BISON
- Validation of pulverization criterion by comparison with existing experimental data is in progress

Gaseous swelling in U-(Pu)-Zr fuels

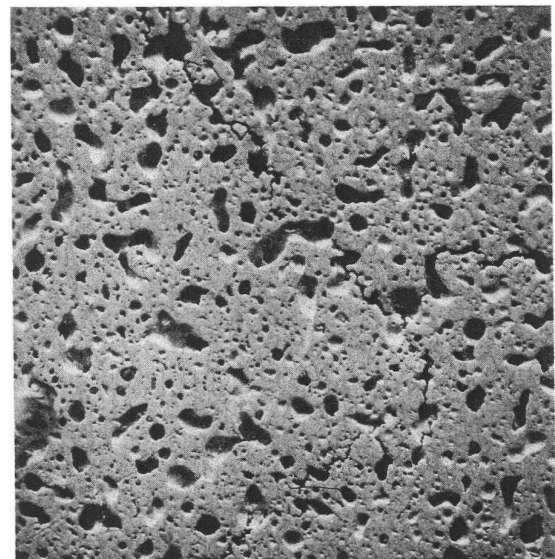
- Renewed interest from commercial sector (Oklo Aurora, Lightbridge)
 - Draw on experience from EBR-II reactor at INL
- Fuel pin center: Gamma + (alpha or beta) phase
 - Gamma-phase swelling and microstructure: Dominated by large fission gas bubbles
- Fuel pin periphery: Alpha + delta phases
 - Swelling primarily due to tearing mechanism
- Current BISON models assume swelling and fission gas release by fission gas bubble mechanism (gamma) throughout



Oklo Aurora



Lightbridge



Gas bubble microstructure in γ phase U-Zr fuel

Hoffman & Walters, Metallic Fast Reactor Fuels

New swelling models added to BISON for U-(Pu)-Zr fuels

- UPuZrGaseousEigenstrain: Single equation analytical model
- Gaseous swelling:

$$\left(\frac{\Delta V}{V_0}\right)_g = \left(\frac{3}{4\pi}\right)^{1/2} \frac{[(kT/2\gamma)Y_{Xe}\dot{F}t]^{3/2}}{N^{1/2}}$$

- T = temperature
- γ = surface energy of bubble-solid interface (have this from lower length scale)
- Y_{Xe} = gaseous fission product yield
- F = fission rate density
- t = time
- N = number density of bubbles (estimated from experimental data)

Threshold for gas release in UPuZrGaseousEigenstrain

- Swelling occurs until porosity is high enough to allow gas release
 - Swelling tapers off linearly in range from $p_i < p < p_t$
 - p_i = interconnection initiating porosity
 - p_t = interconnection terminating porosity
- Fraction of gas released increases linearly in same range
- Previous estimate of $p_t = 0.25$ porosity (33% swelling) based on analytical estimate (Barnes, JNM, 11, 2, 135-148, 1964). p_i was chosen at 0.23 for model performance rather than physical grounds
- Goal: Develop improved estimates of gas p_i and p_t by simulating percolation of growing fission gas bubbles

Phase-field simulation of growing gas bubbles

- Large 3D simulations required to get good statistics, so start with the simplest model possible
 - Cahn-Hilliard model, single defect species with source term for production in the solid
 - Free energy with minima at normalized defect concentrations $c = 0$ and $c = 1$

$$F = \int_v (f_b + f_{grad}) dV \quad f_b = W c^2 (1 - c)^2 \quad f_{grad} = \frac{\kappa}{2} |\nabla c|^2$$

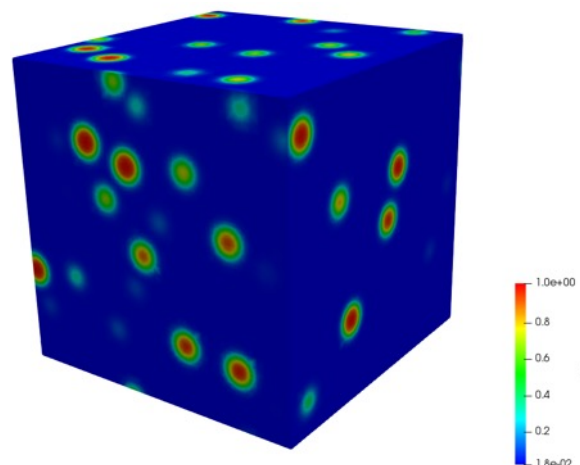
$$\mu = \frac{\delta F}{\delta c} = \frac{\partial f_b}{\partial c} - \kappa \nabla^2 c$$

$$\frac{\partial c}{\partial t} = \nabla \cdot (M \nabla \mu) + S$$

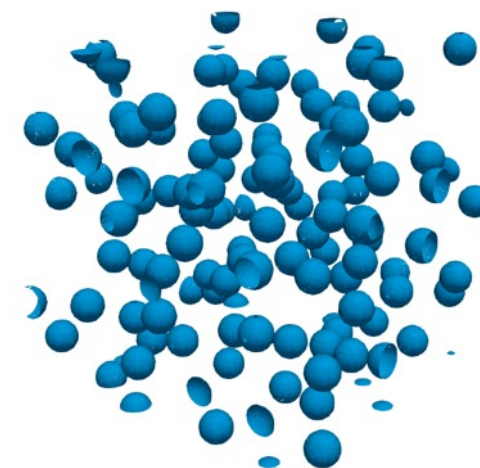
$$S = s_0 [1 - h(c)]$$

Phase-field simulation of growing gas bubbles

- Initial conditions: Randomly placed isolated bubbles at $N = 3 \times 10^{14}/\text{m}^3$, as determined from experiment
- Interfacial energy 1.8 J/m^2 from atomistic calculations
- Diffusivity not well known, so vary parametrically with fixed source strength to see effect



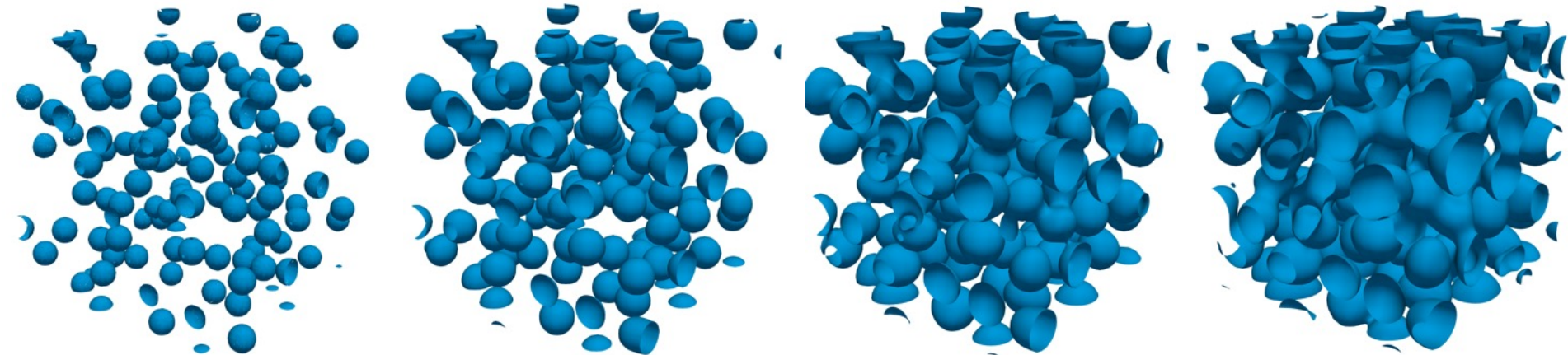
Initial conditions, simulation volume $(72 \mu\text{m})^3$



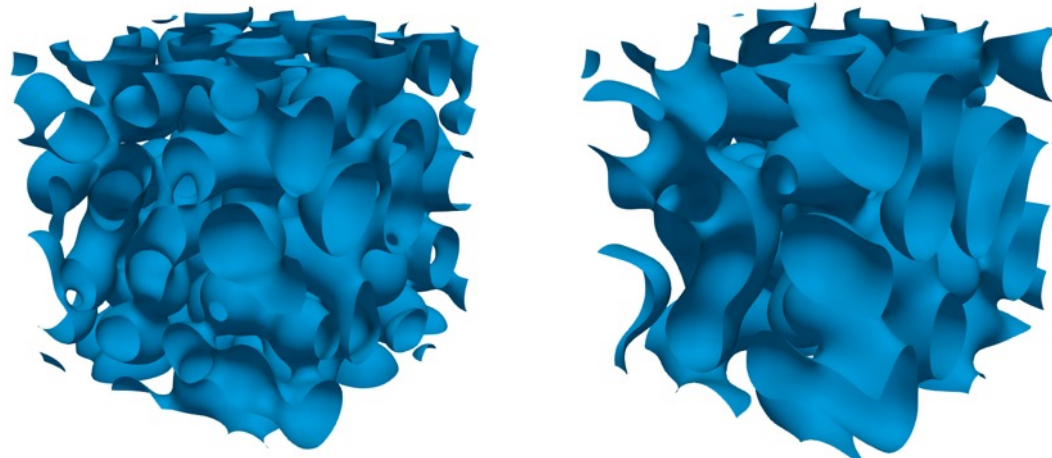
$c = 0.5$ contour

Phase-field simulation results

- $(72 \text{ }\mu\text{m})^3$ domain, 112 bubbles for $N = 3 \times 10^{14}/\text{m}^3$
- Time evolution for $D = 2 \text{ nm}^2/\text{s}$:



- Effect of diffusivity on morphology:



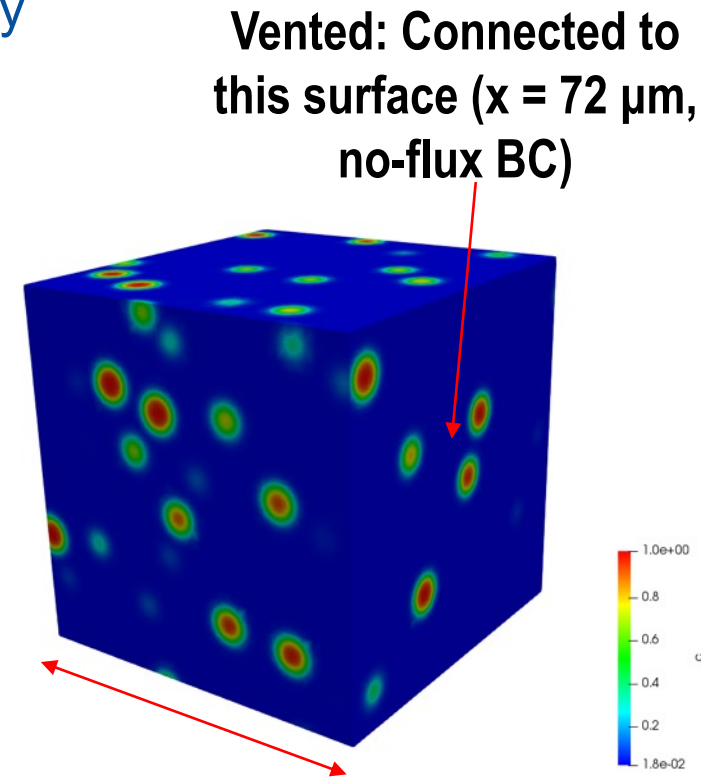
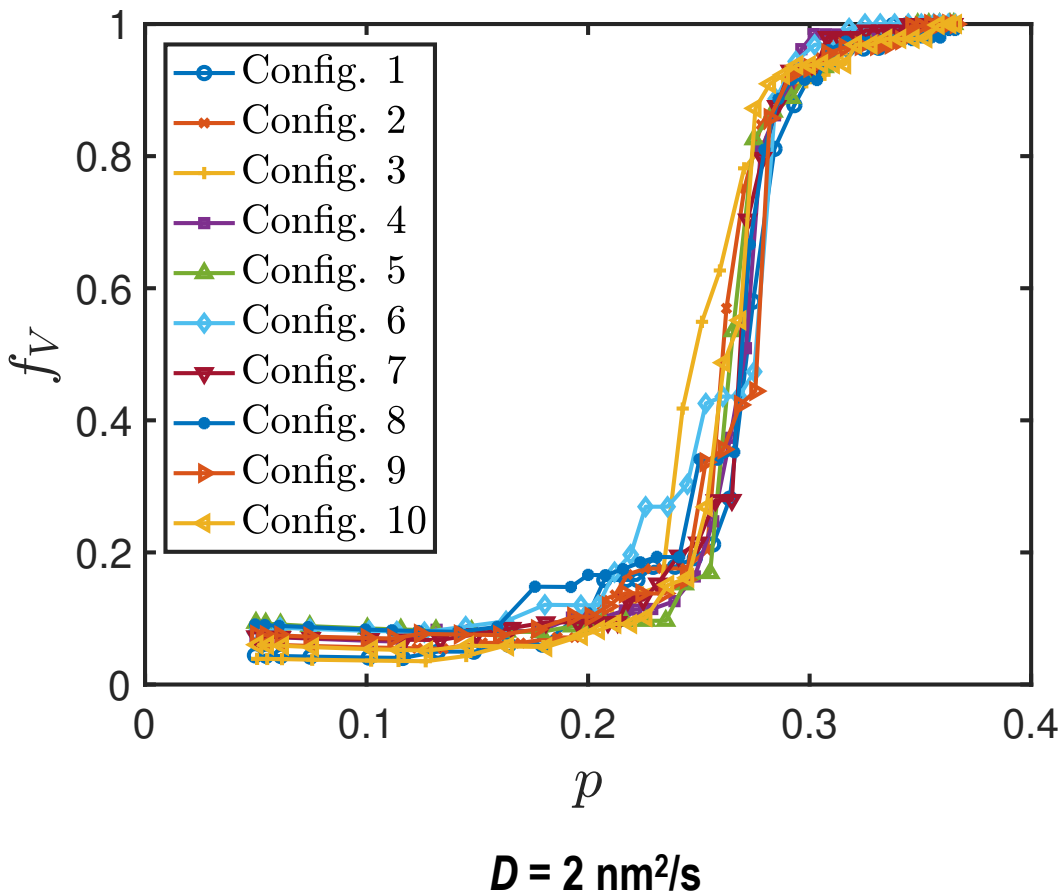
$D = 2 \text{ nm}^2/\text{s}, t = 1.14 \times 10^8 \text{ s}$

$D = 10 \text{ nm}^2/\text{s}, t = 1.14 \times 10^8 \text{ s}$

IDaho National Laboratory

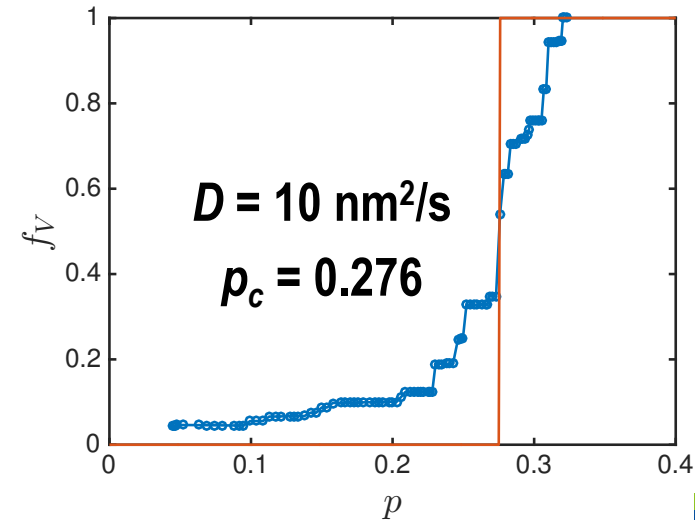
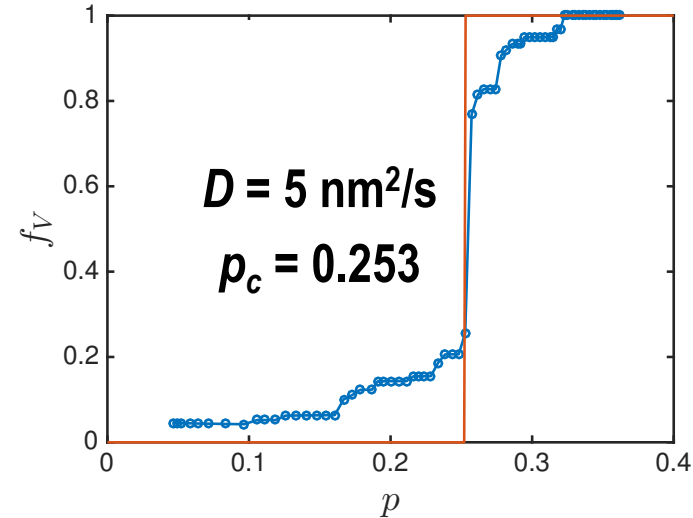
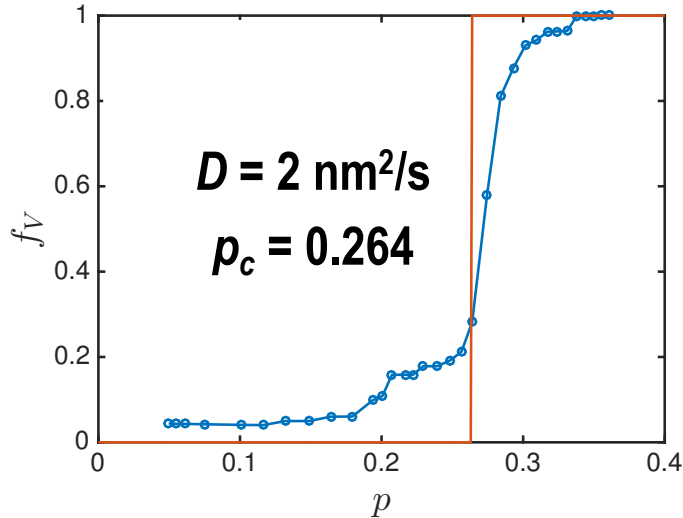
Connectivity to surface

- Fraction vented to surface as a function of porosity
- Percolation threshold (p_c) for each mobility



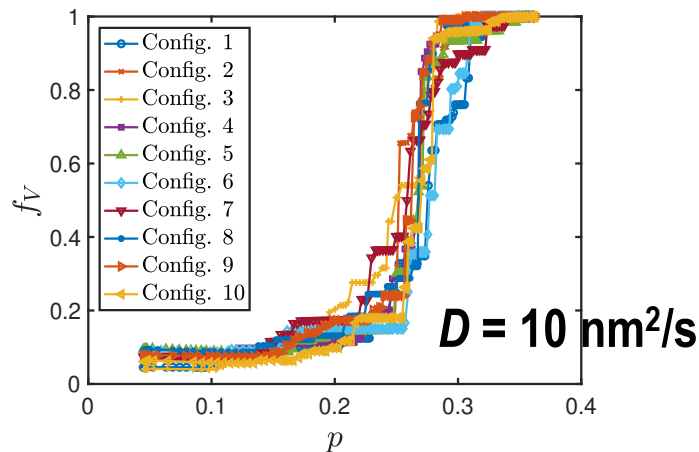
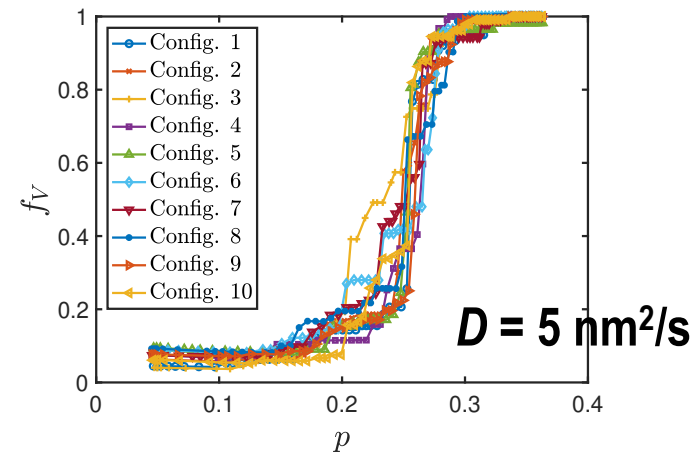
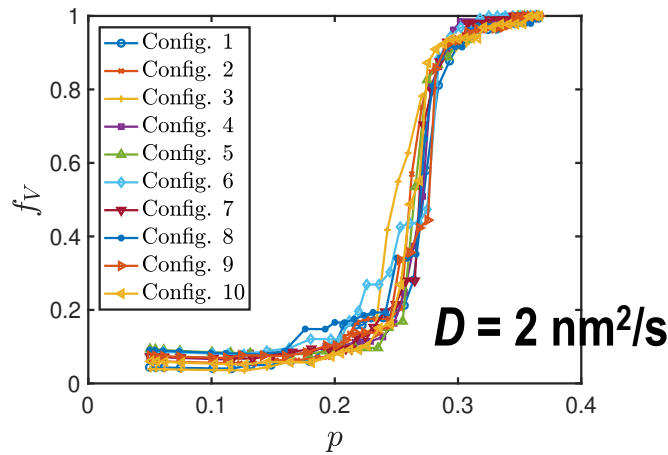
Percolation threshold

- Determined percolation threshold p_c for each mobility



Varying initial conditions to obtain improved statistics and quantify uncertainty

- Generated multiple random bubble distributions for initial conditions



$D (\text{nm}^2/\text{s})$	$N (\text{m}^{-3})$	Mean p_c	Std. dev. p_c
2	3×10^{14}	0.263	0.0101
5	3×10^{14}	0.254	0.00902
10	3×10^{14}	0.265	0.00922

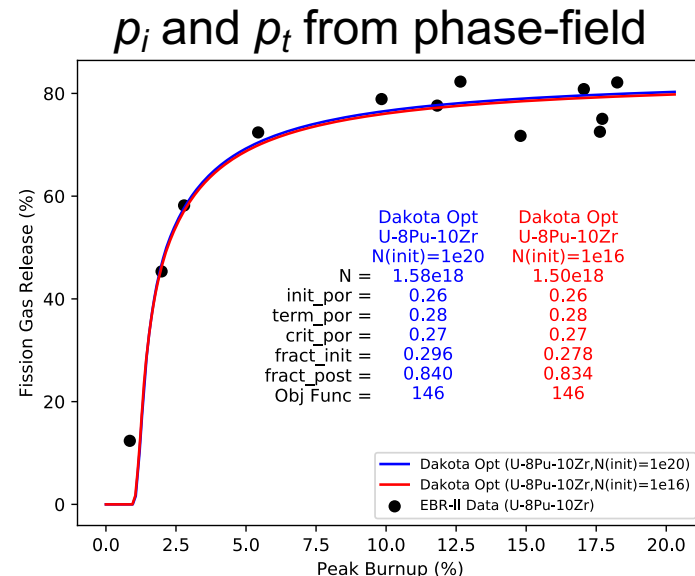
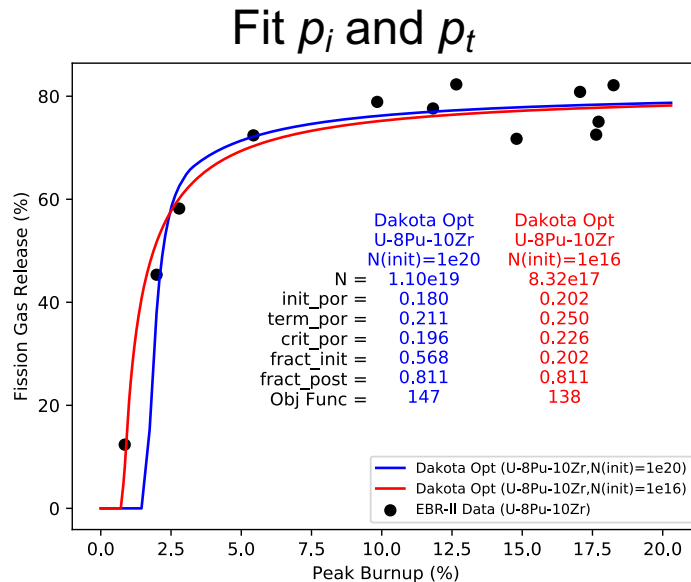
Determining parameters for Bison U-(Pu)-Zr swelling model

- Assume no significant gas release can occur from interior regions of fuel until percolation threshold is reached
 - Set $p_i = \text{mean } p_c = 0.262$
- Based on EBR-II post-irradiation examination, fission gas release plateaued at 80% of fission gas produced
 - Define $p_{0.8}$ as the porosity at which $f_V = 0.8$
 - Set $p_t = \text{mean } p_{0.8} = 0.28$

D (nm²/s)	Mean $p_{0.8}$	Std. dev. $p_{0.8}$
2	0.280	0.00407
5	0.272	0.0103
10	0.283	0.0120

BISON fission gas release prediction from simulated EBR-II fuel pin

- Optimization was performed using Dakota to determine model parameters that best matched experimental measurement of FGR
 - Results were strongly dependent on initial guesses for parameters
- Using values of p_i and p_t from phase-field simulations significantly reduced the dependence on initial guesses for other parameters



Conclusions and next steps

- Determined improved parameters for BISON model UPuZrGaseousEigenstrain
 - Results fairly consistent for varying defect species mobility (over limited range considered)
 - Higher initial bubble density pushed percolation and venting earlier
 - Further efforts to quantify this parameter (experiment and simulation) for a variety of fuel compositions and operating conditions
- More advanced swelling model development in progress (considers more realistic gas equation of state, effect of hydrostatic stress, more realistic interconnectivity function)
 - Same simulations are being analyzed to parameterize this model

Parameterization of BISON model for fission gas release in U_3Si_2 nuclear fuel using phase- field simulations

Larry Aagesen¹, David
Andersson², Benjamin Beeler³,
Michael W.D. Cooper², Kyle
Gamble¹, Yinbin Miao⁴, Giovanni
Pastore⁵, Cody Permann¹,
Michael Tonks⁶

¹Idaho National Laboratory

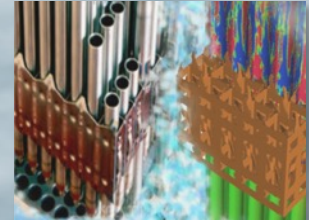
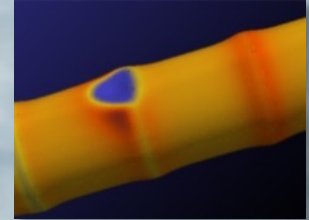
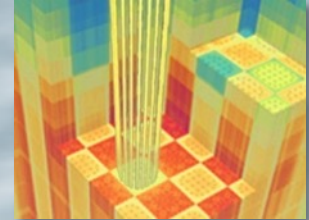
²Los Alamos National Laboratory

³North Carolina State University

⁴Argonne National Laboratory

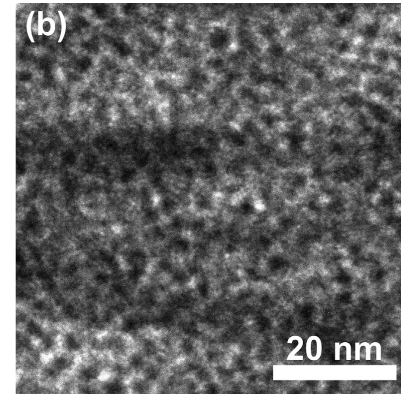
⁵University of Tennessee

⁶University of Florida

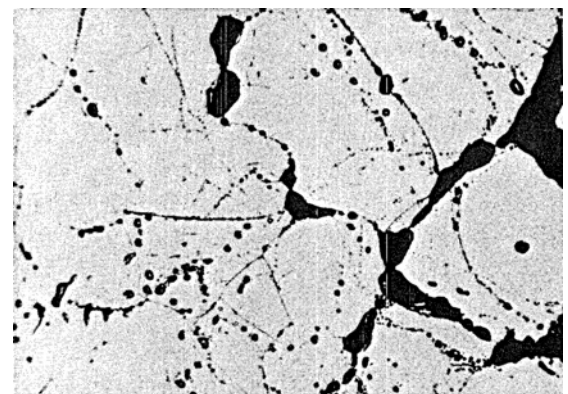


U_3Si_2 is being considered as a potential accident-tolerant fuel

- Compared with UO_2 :
 - Lower melting temperature
 - But higher thermal conductivity may give higher margin to melting temperature
- U_3Si_2 swelling/fission gas release behavior less well characterized
 - Evidence from higher-temperature irradiation suggests pellet-form fuel would remain crystalline, have similar microstructure as UO_2 fuel
- BISON model recently developed based on these assumptions

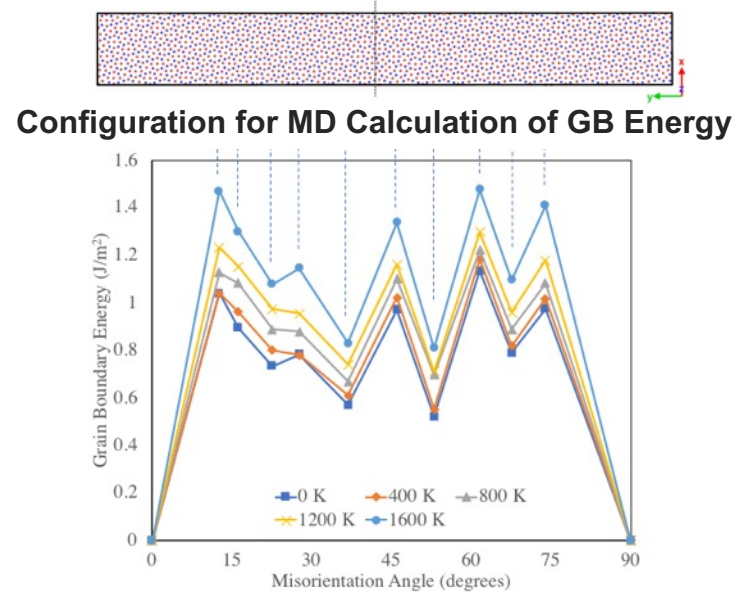
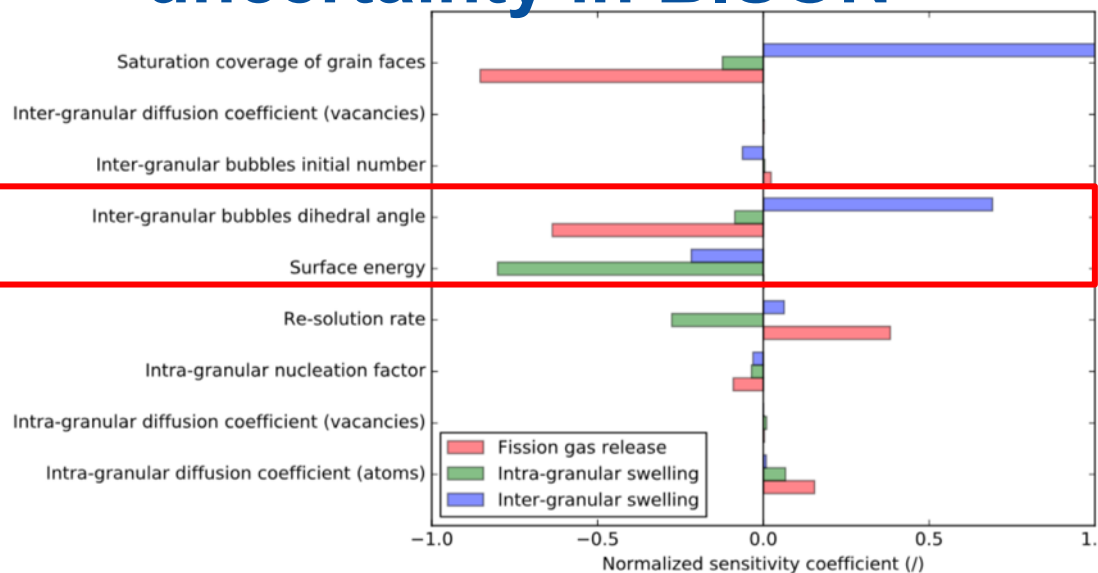


U_3Si_2 implanted with Xe at 873 K
(Miao et al., J. Nuclear Mater., 503, 314-322 (2018)).



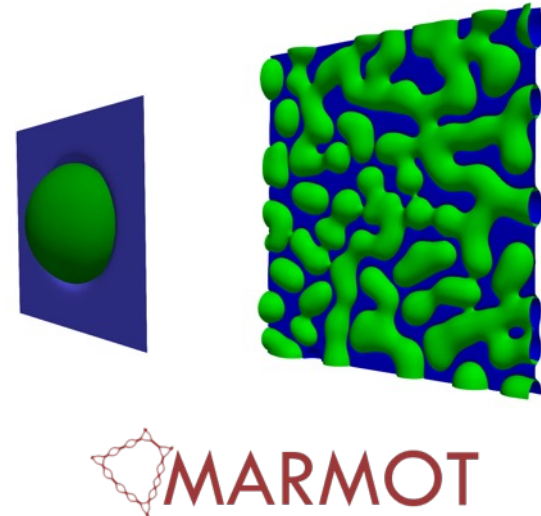
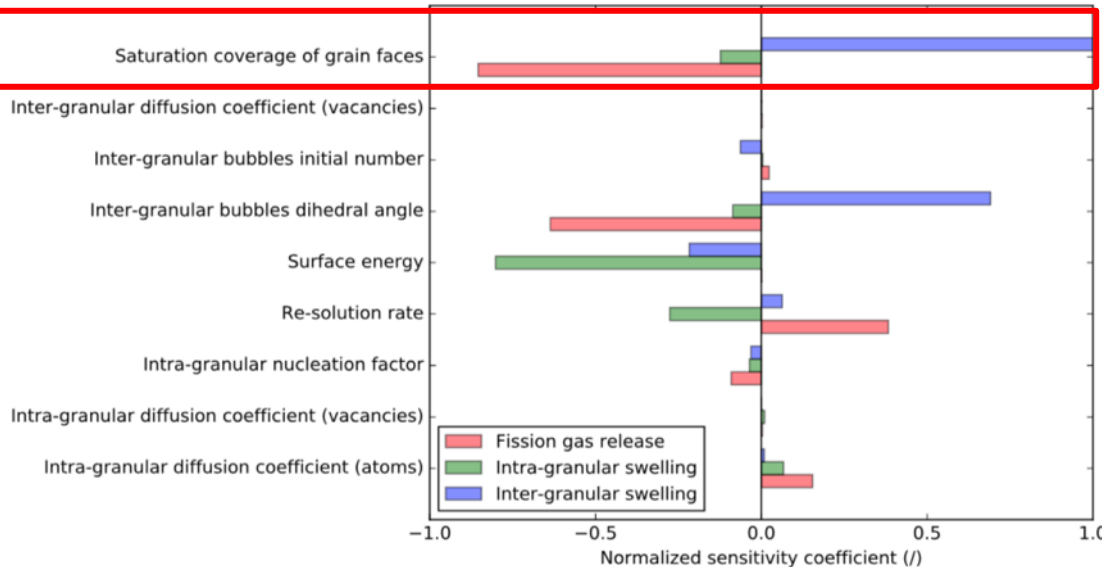
U_3Si_2 irradiated at ~950 K and ~6 GWd/tU (Shimizu, NAA-SR-1062, 1965).

Lower length scale calculations to reduce uncertainty in BISON



- Sensitivity analysis of BISON U₃Si₂ swelling and gas release predictions showed strong dependence on inter-granular bubble dihedral angle and surface energy
 - Measured values also not available
- Surface energy and grain boundary energies were determined for U₃Si₂ using molecular dynamics (MD) calculations
 - Dihedral angle (θ) calculated from surface energy and grain boundary energy; input to BISON
 - Data also used to parameterize Marmot model

Lower length scale calculations to reduce uncertainty in BISON

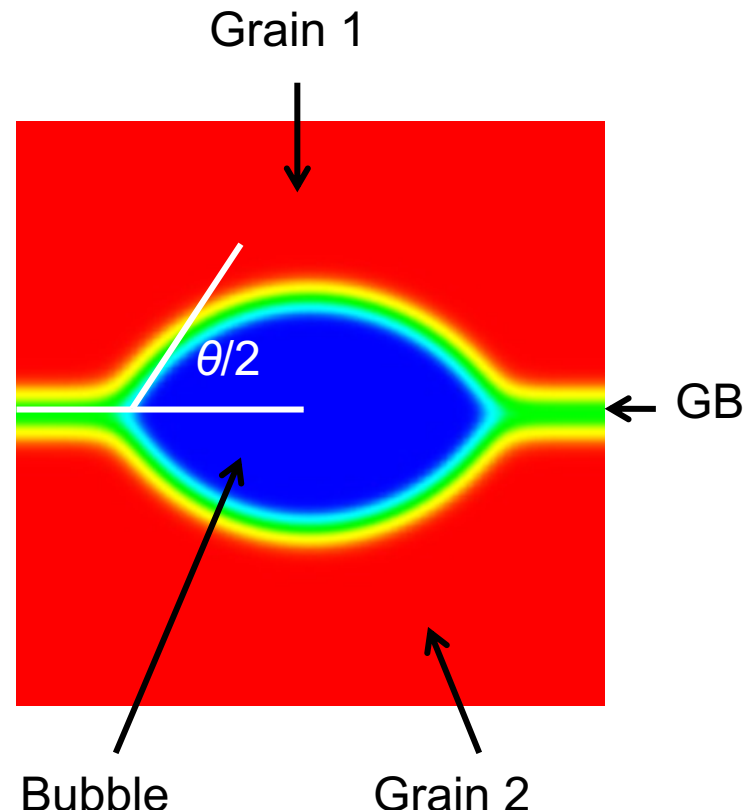


- Sensitivity analysis also showed strong dependence on saturation coverage of grain faces ($F_{c,sat}$)
 - No measured value available for U_3Si_2
- Phase-field simulations¹ showed progress of grain boundary venting was strongly dependent on intergranular bubble areal density and dihedral angle
 - New phase-field simulations are being used to determine $F_{c,sat}$ using U_3Si_2 parameters

¹Millett, Tonks, Biner, L. Zhang, Chockalingham, Y. Zhang, *J. Nucl. Mater.*, 425, 130-135 (2012).

Phase-field model: Essential physics

- Represent bubble phase and multiple grains of U_3Si_2
- Track vacancies and fission product species (Xe only)
 - Source terms for production
- Set surface energy and grain boundary energy
 - Controls dihedral angle θ
 - Remove bulk energy contribution to interfacial energy



Phase-field model: Grand-potential functional

$$\Omega = \int_V \left(m \left[\sum_{\alpha} \sum_{i=1}^{p_{\alpha}} \left(\frac{\eta_{\alpha i}^4}{4} - \frac{\eta_{\alpha i}^2}{2} \right) + \sum_{\alpha} \sum_{i=1}^{p_{\alpha}} \left(\sum_{\beta} \sum_{j=1, \alpha i \neq \beta j}^{p_{\beta}} \frac{\gamma_{\alpha i \beta j}}{2} \eta_{\alpha i}^2 \eta_{\beta j}^2 \right) + \frac{1}{4} \right] + \frac{\kappa}{2} \sum_{\alpha} \sum_{i=1}^{p_{\alpha}} |\nabla \eta_{\alpha i}|^2 + \sum_{\alpha} h_{\alpha} \omega_{\alpha} \right) dV$$

- Multi-phase, multi-order parameter extension to grand-potential model
- Advantages:
 - Bulk free energy contribution is removed from interfacial energy
 - Allows interfacial thickness and energy to be set independently, enabling coarser mesh, improved computational performance
 - Similar to KKS in this respect, but do not need separate phase concentration variables, so performance is improved
 - Prevents spurious formation of additional phases at two-phase interfaces

Phase-field model evolution equations

- Order parameters: Allen-Cahn
- Densities: Change to chemical potential for each species

Gas:

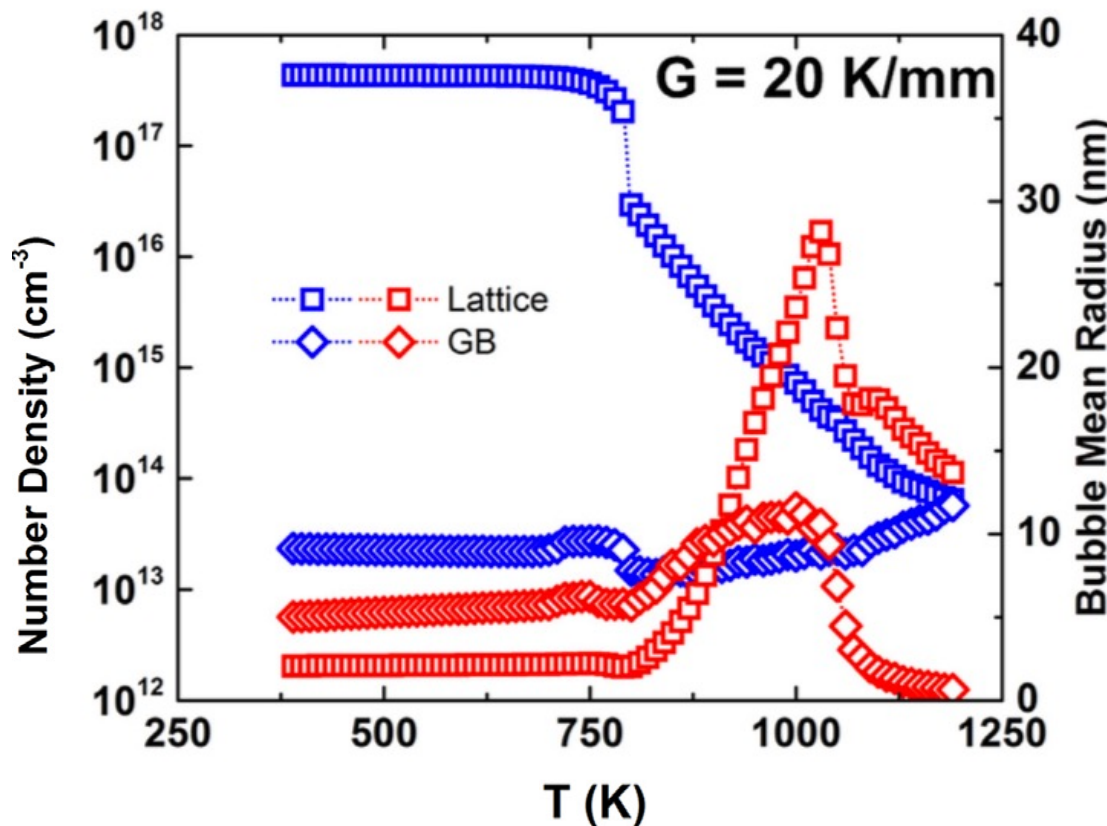
$$\frac{\partial \mu_g}{\partial t} = \frac{1}{\chi_g} \left[\nabla \cdot (D_g \chi_g \nabla \mu_g) + s_g - \sum_{\alpha} \sum_{i=1}^{p_{\alpha}} \frac{\partial \rho_g}{\partial \eta_{\alpha i}} \frac{\partial \eta_{\alpha i}}{\partial t} \right]$$

Vacancies:

$$\frac{\partial \mu_v}{\partial t} = \frac{1}{\chi_v} \left[\nabla \cdot (D_v \chi_v \nabla \mu_v) + s_v - \sum_{\alpha} \sum_{i=1}^{p_{\alpha}} \frac{\partial \rho_v}{\partial \eta_{\alpha i}} \frac{\partial \eta_{\alpha i}}{\partial t} \right]$$

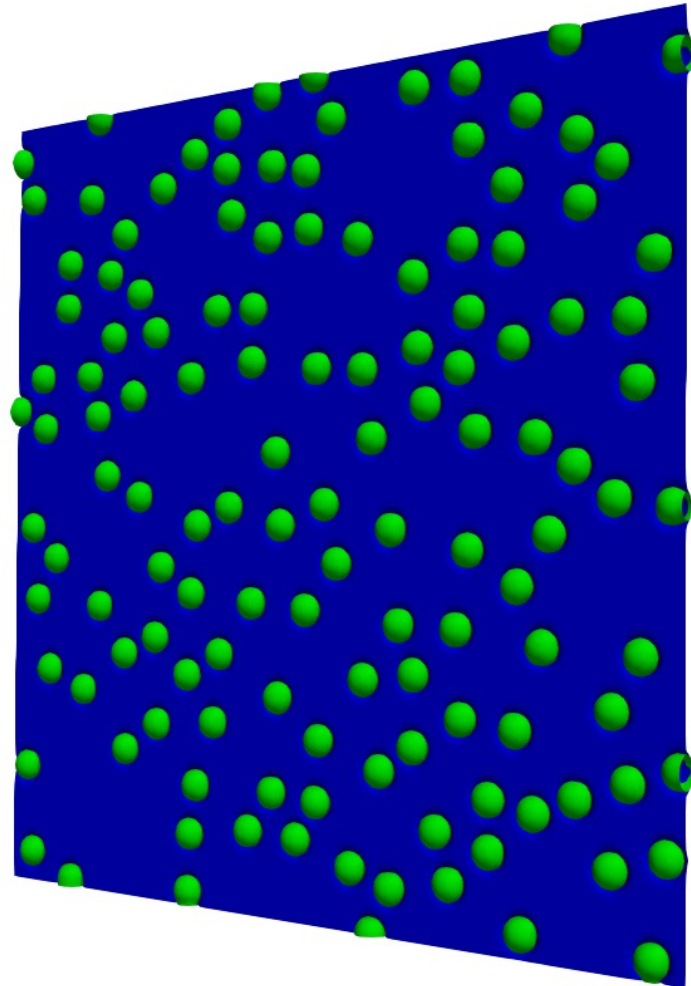
Phase-field model initial conditions

- Intergranular bubble areal density (n_a): Determine from rate theory simulations
 - At 1035 K, $n_a = 15 / \mu\text{m}^2$



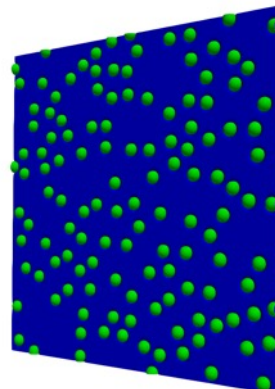
Phase-field model initial conditions

- Determine $F_{c,sat}$
- 1035 K
- $\theta/2 = 73$
- No-flux boundary conditions
- $3 \mu\text{m} \times 3 \mu\text{m}$ grain boundary
- Populate with randomly placed lenticular bubbles, $n_a = 15 / \mu\text{m}^2$, minimum spacing 160 nm

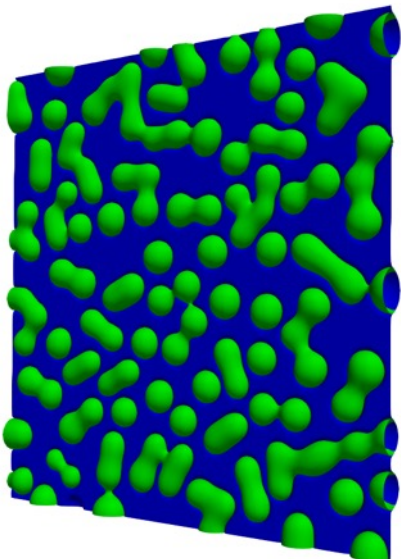


$3 \mu\text{m} \times 3 \mu\text{m}$

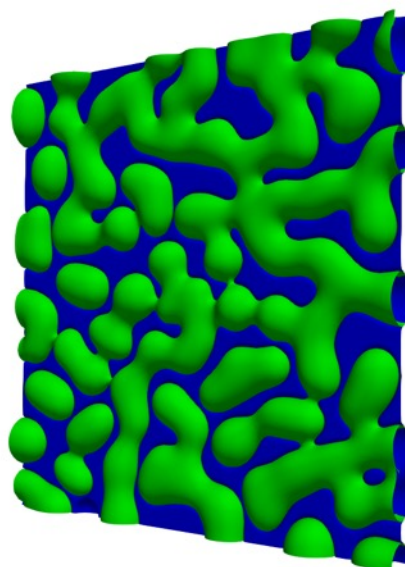
Phase-field simulation results



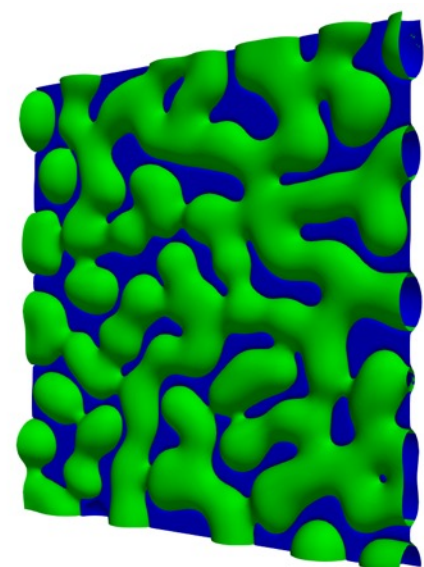
$t = 0$



$t = 6.04 \times 10^7$ s

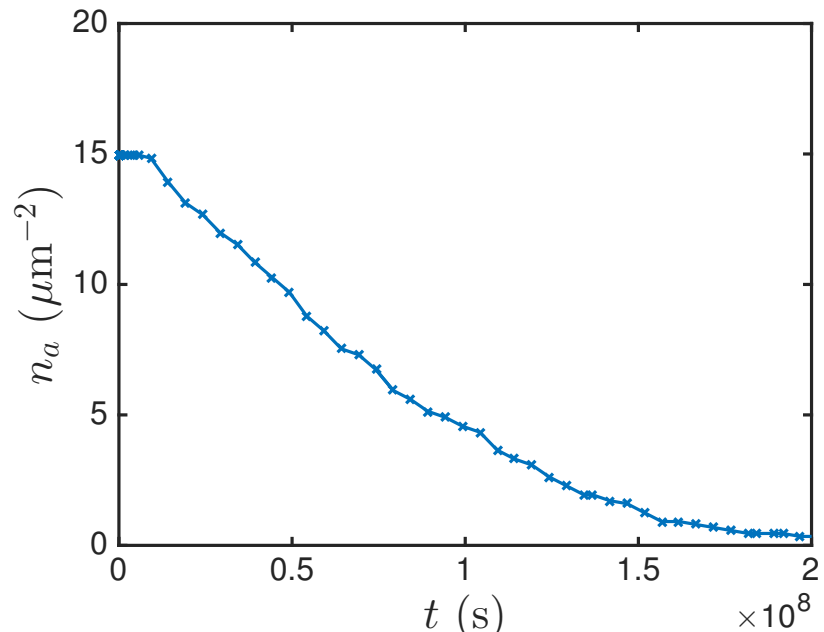
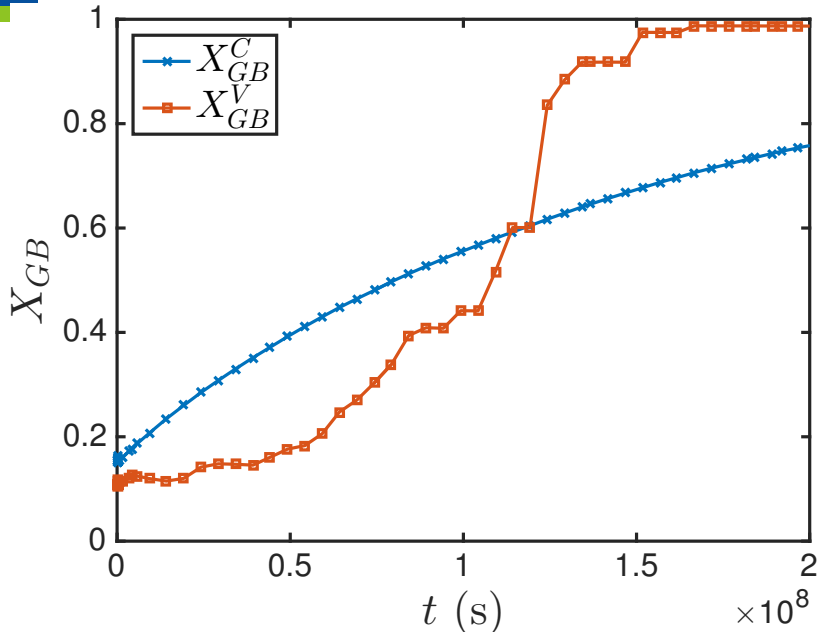


$t = 1.62 \times 10^8$ s



$t = 1.97 \times 10^8$ s

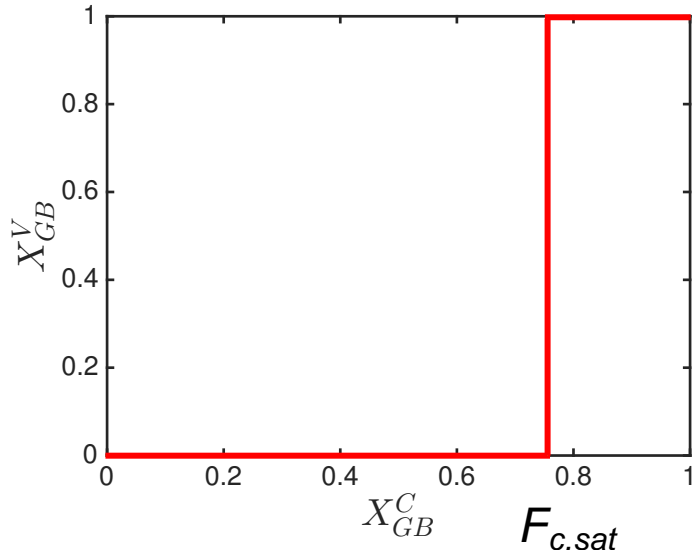
Phase-field simulation results



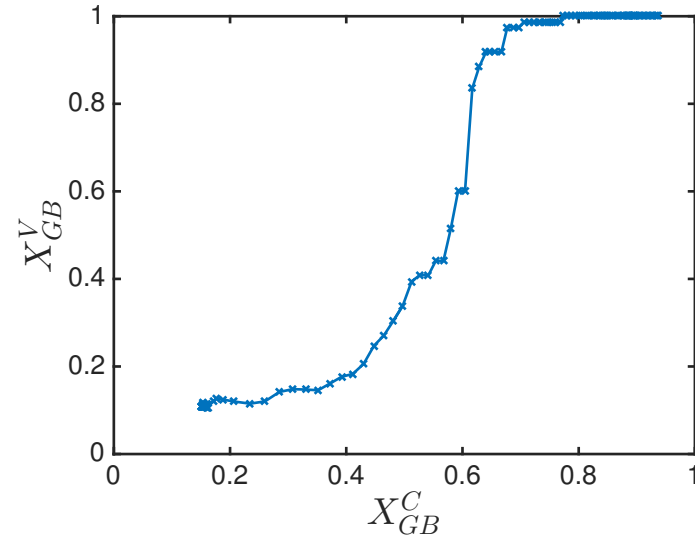
- Plot fractional coverage of GB (X_{GB}^C) and fraction of bubbles that are vented to edge of domain (X_{GB}^V) vs. time
 - Less rapid increase with respect to time compared to previous simulations of Millett et al., due to slow buildup from source terms
- Areal density of bubbles vs. time
 - Rate of coalescence relatively constant until the bubble density reaches approximately half its initial value, then slows

Informing BISON with phase-field results

- Plot fraction of bubbles that are vented to edge of domain (X_{GB}^V) vs. fractional coverage of GB (X_{GB}^C)
- Implications for BISON:
 - Short term: Set $F_{c,sat}$ where slope of curve is greatest (shown: $X_{GB}^C = 0.62$)
 - Longer term: Modify BISON model to turn off swelling and release gas gradually following curve shape



Previous BISON Assumption



Marmot Simulation

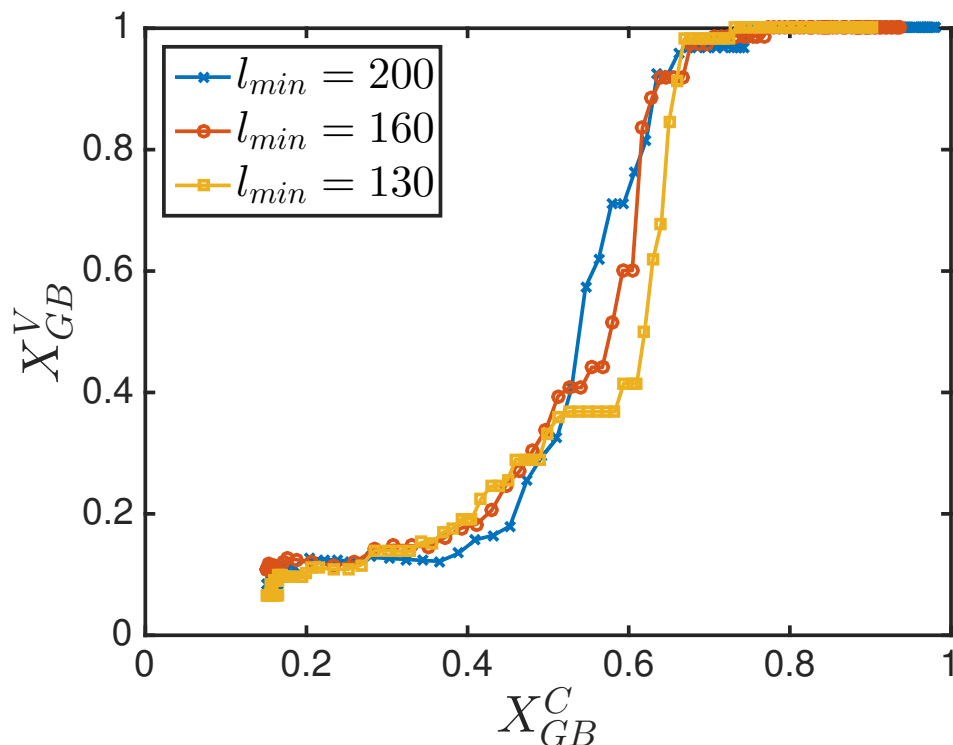
Effect of simulation assumptions on predicted value for BISON model

- Simulation initial conditions
 - Maintain all simulation parameters the same, including minimum spacing $l_{min} = 160 \text{ nm}$
 - Change seed in random number generator used to determine initial bubble positions
 - 5 total configurations simulated using these parameters
- Mean $F_{c,sat} = 0.60$
- Standard deviation indicates calculated value of $F_{c,sat}$ is relatively insensitive to initial bubble configuration

Configuration	$F_{c,sat}$
1	0.54
2	0.62
3	0.61
4	0.63
5	0.62
Mean	0.60
Standard Deviation	0.036

Effect of minimum bubble spacing in initial conditions

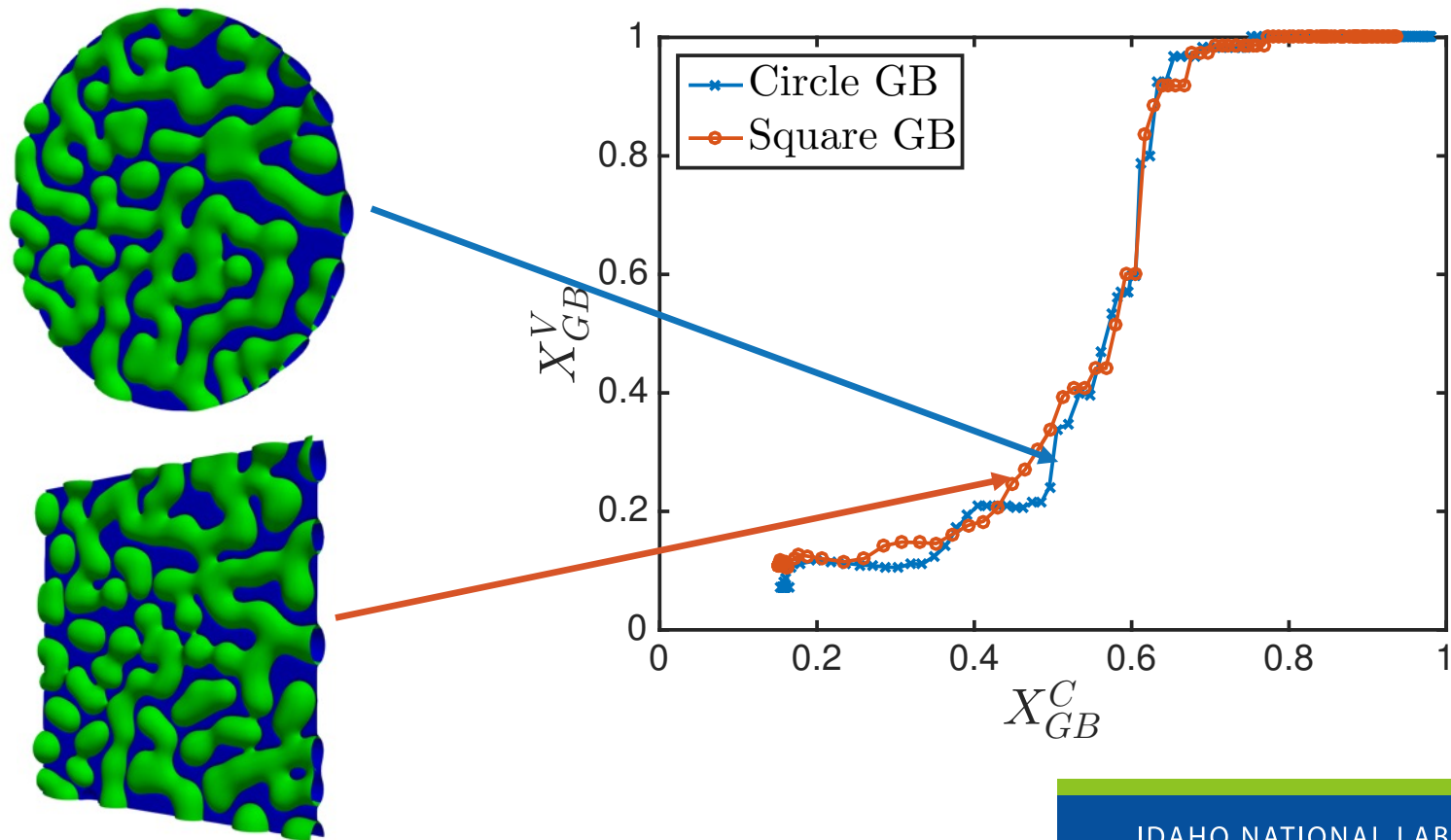
- Also simulated $l_{min} = 130 \text{ nm}, 200 \text{ nm}$, 5 configurations each
- 200 nm: Initial portion of release curve delayed
- Slight decrease in $F_{c,sat}$ with l_{min} , but may be just due to statistical variation



Min. spacing (l_{min}), nm	$F_{c,sat}$
130	0.61 ± 0.039
160	0.60 ± 0.036
200	0.58 ± 0.046

Effect of simulation domain geometry

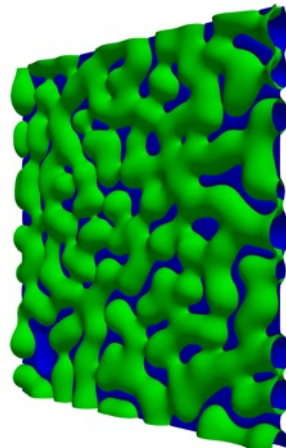
- Compare venting curves for circular GB vs. square GB
 - Circular GB: $F_{c,sat} = 0.61 \pm 0.046$, Square GB: 0.60 ± 0.036
 - Conclude that GB geometry does not have a significant effect



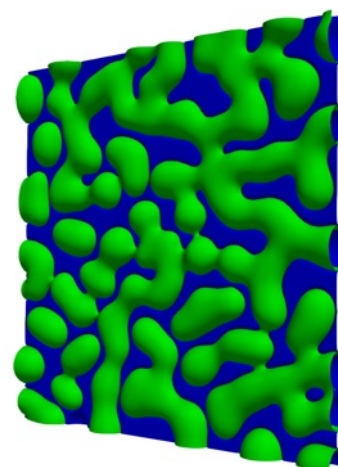
Effect of simulation temperature

- Current BISON model assumes $F_{c,sat}$ is independent of temperature
- Primary effect of varying temperature: Gas diffusivity D_g
- Ran 5 simulations with $T = 1015$ K (D_g decreased by 2x)
 - Much finer microstructure at same simulation time
 - No change in calculated $F_{c,sat} = 0.60 \pm 0.014$

Microstructure at
 $t = 1.98 \times 10^8$ s:



$$D_g = 0.05 \text{ nm}^2/\text{s}$$



$$D_g = 0.1 \text{ nm}^2/\text{s}$$

Conclusions: U₃Si₂ fission gas release

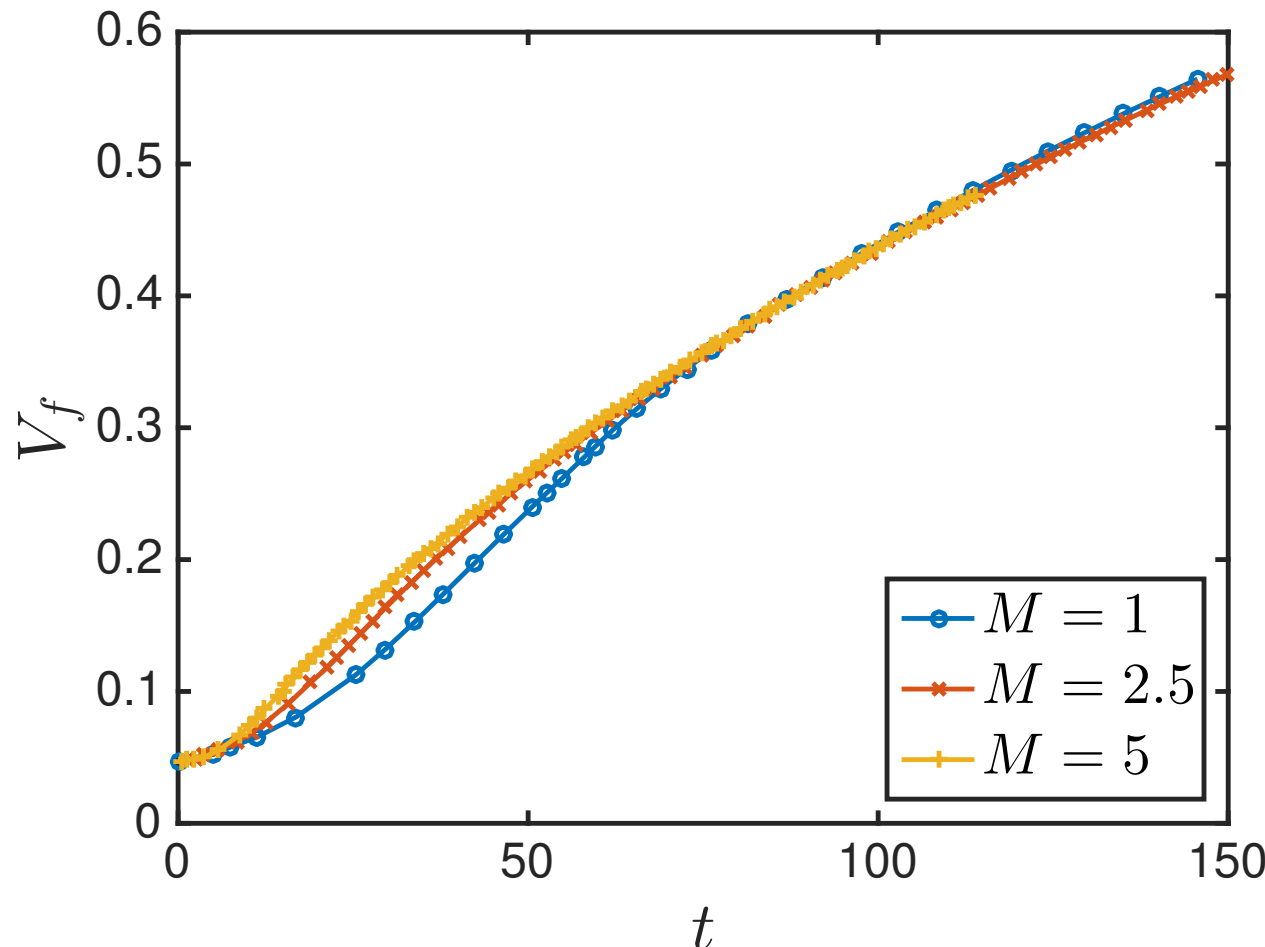
- BISON predictions of fission gas release and swelling are strongly dependent on dihedral angle, surface energy, $F_{c,sat}$
 - No measured values available
- Phase-field simulations were used to calculate $F_{c,sat}$
 - Determined without needing to wait for costly post-irradiation examination
- $F_{c,sat} = 0.60$ recommended for BISON U₃Si₂ model
- No strong effect on $F_{c,sat}$ from initial conditions, minimum bubble spacing, simulation domain geometry, temperature (in range considered)
- New value of $F_{c,sat}$ was used in BISON simulations of U3Si2 irradiated in the Advanced Test Reactor at INL. Use of the LLS-determined improved predictions of fuel elongation and fission gas release compared to the previously used value $F_{c,sat} = 0.78$ (based on theoretical analysis)

Thank you!
Funding Support: DOE-NE
NEAMS Program



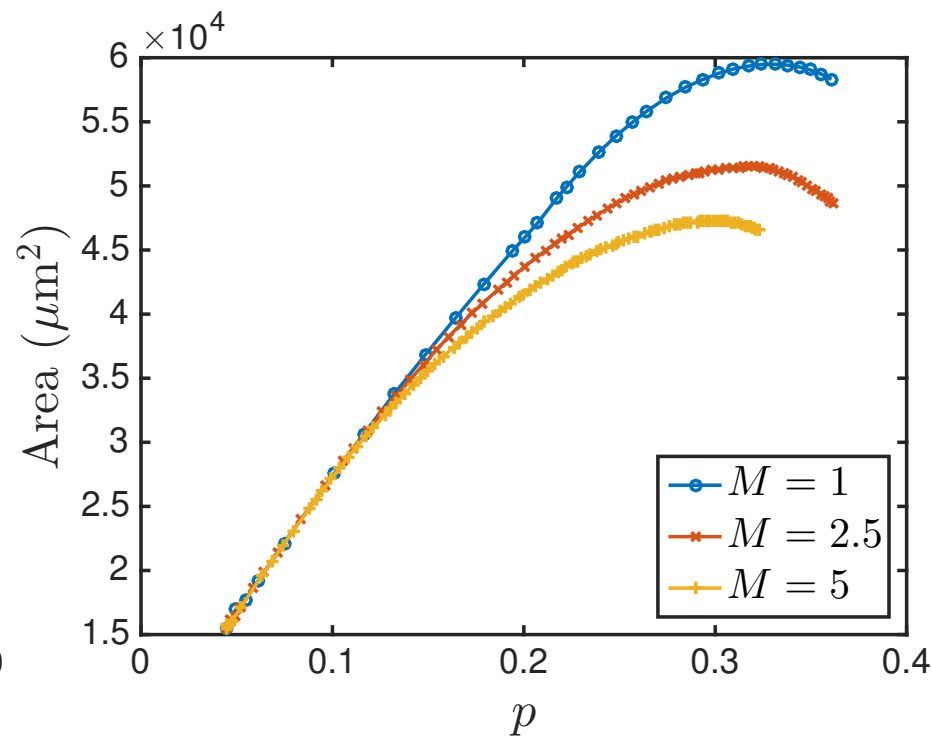
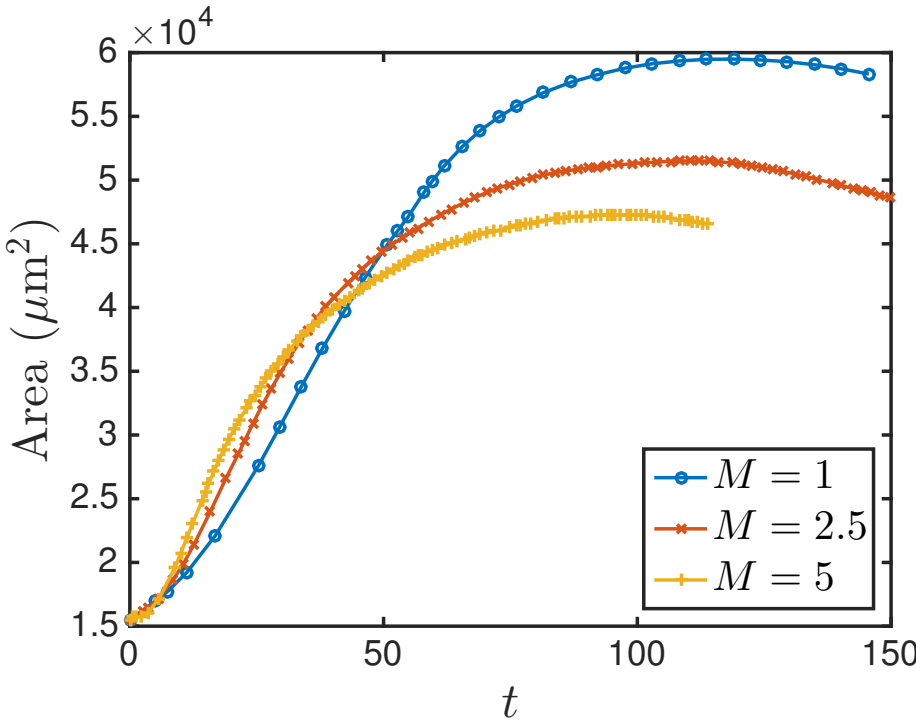
Questions?

Volume fraction of bubble phase



- High M : Volume fraction increases more quickly as defect species is carried from solid to bubbles more quickly

Surface area of interface



- Mobility changes morphology
 - Competition between source term growth (increases surface area) and coarsening (reduces surface area)
 - High mobility case: Coarsening is accelerated, reducing surface area as growing bubbles begin to interact with each other

Length scale/feature size

- Would like to have simulation domain size \gg length scale throughout
- How to measure?
 - Bubble radius is convenient in early stages but loses meaning when a highly interconnected microstructure forms
 - Alternative: Inverse of surface area per unit volume of bubble phase, $1/S_v$
 - Used for coarsening in past
 - $1/S_v$ remains at least an order of magnitude $<$ domain size ($72 \mu\text{m}$) throughout

